J Neurophysiol 125: 938–956, 2021.
First published February 10, 2021; doi:10.1152/jn.00530.2020

american physiological society

JNP JOURNAL OF NEUROPHYSIOLOGY

REVIEW

Magnetoencephalography: physics, techniques, and applications in the basic and clinical neurosciences

Junseok A. Kim[1,2] and Karen D. Davis[1,2,3]

[1]*Division of Brain, Imaging and Behaviour, Krembil Brain Institute, Krembil Research Institute, University Health Network, Toronto, Ontario, Canada;* [2]*Institute of Medical Science, Faculty of Medicine, University of Toronto, Toronto, Ontario, Canada; and* [3]*Department of Surgery, University of Toronto, Toronto, Ontario, Canada*

Abstract

Magnetoencephalography (MEG) is a technique used to measure the magnetic fields generated from neuronal activity in the brain. MEG has a high temporal resolution on the order of milliseconds and provides a more direct measure of brain activity when compared with hemodynamic-based neuroimaging methods such as magnetic resonance imaging and positron emission tomography. The current review focuses on basic features of MEG such as the instrumentation and the physics that are integral to the signals that can be measured, and the principles of source localization techniques, particularly the physics of beamforming and the techniques that are used to localize the signal of interest. In addition, we review several metrics that can be used to assess functional coupling in MEG and describe the advantages and disadvantages of each approach. Lastly, we discuss the current and future applications of MEG.

magnetoencephalography; MEG; oscillations

PHYSICS OF MAGNETOENCEPHALOGRAPHY

Measuring the Signal

The principle of measuring brain signals with magnetoencephalography (MEG) lies in the basic physics principle that a moving current creates a magnetic field based on the right hand rule (1). The measured magnetic field in MEG is generated by postsynaptic potentials, intracellular longitudinal currents, cell discharges, synchronized slow currents, subthreshold oscillations, and postspike after potentials (2–5). It is tricky to estimate the magnitude, orientation, and position of the underlying electrical currents from the extracranially measured magnetic field and this is known as an "ill-posed" inverse problem, which has a potentially infinite number of possible solutions (6). Much of the cortical signal that we can measure with MEG is believed to arise from the neocortical sheet and only the current sources with a tangential can be measured (i.e., mainly in the fissures of the brain) (3). However, the proportion of cortical sheet that is not resolvable is thought to be quite small (<5%) (7), and empirical work shows that some radial sources (e.g., from lateral surface of the brain) can still be measured in the brain using the MEG (8). The issue of radial sources will be further discussed in later sections. The magnetic fields being measured (on the order of 10^{-12} to 10^{-15} Tesla) are infinitesimally weak compared with the earth's magnetic field (on the order of 10^{-4} to 10^{-5} Tesla) and even that of the heart and muscle (9). The challenge, therefore, for MEG systems to measure brain signals is the process of isolating miniscule brain-related signals from the massively greater signals from outside the brain. Thus, MEG has required the development of very exquisitely sensitive sensors, filtering, and a method to shield the sensors from recording outside noise (Fig. 1).

Currently, conventional MEG systems are cryogenic and use sensitive magnetic field sensors called superconducting quantum interference devices or SQUIDs (Fig. 2) (10–12). SQUIDs are made from materials that become superconductors at extremely low temperatures, meaning that the material can conduct electricity without resistance. Another feature that distinguishes the SQUID from a conventional superconductor is the presence of one or more Josephson junction (depending on the type of SQUID). The Josephson junction consists of two superconductors separated by an insulating barrier and is essential for the Josephson effect to occur inside the SQUID (13). Many of the MEG systems today use niobium for the SQUIDs because it can reliably reach a superconductive state at low temperatures and return back to room temperature.

The basic process of measuring a signal in MEG can be divided into several steps (3, 14). First, a magnetic field from the brain is detected by the pick-up coil. A pick-up coil is much larger in diameter than the SQUID to increase the efficiency of

Correspondence: K. D. Davis (karen.davis@uhnresearch.ca).
Submitted 2 September 2020 / Revised 19 January 2021 / Accepted 20 January 2021

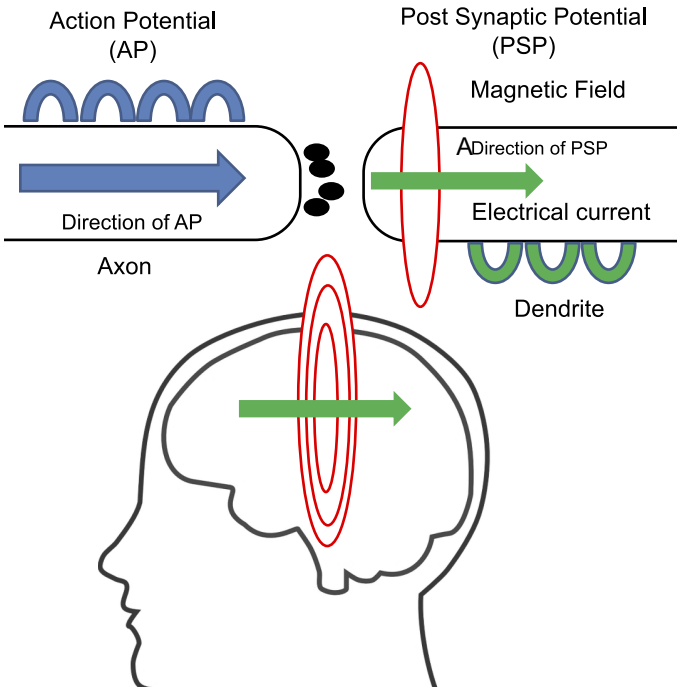

Figure 1. The origin of MEG signals. The red circles depict the magnetic field that is induced from the cumulative electrical current (green arrow) of the postsynaptic potentials that are measured by the MEG. The blue arrow indicates the direction that action potentials propagate. MEG, magnetoencephalography.

detection. There are two types of pick-up coils currently used in MEG systems: the magnetometer and the gradiometer. Of the two types of coils, magnetometers have superior sensitivity to detect shallow and deep sources but they are more prone to picking up outside noise. Thus, magnetometers are most optimal in settings with limited sources of outside noises (i.e., countryside laboratory with no traffic and electrical interference). In contrast, gradiometers are less sensitive to outside noise, which makes them the superior option in locations with a number of large-sized electronical devices (e.g., a busy hospital). There are two types of gradiometers: axial and planar. Of the two variations, axial gradiometers are more sensitive at measuring deep sources (~5 times the signal strength on 8-cm depth sources), while planar gradiometers are more sensitive at measuring the shallow sources (15).

Pick-up coils are linked to the SQUID by an input coil and are kept in a superconducting state by liquid helium at ~4 K (approximately −269°C). The SQUID then produces a small voltage current that can be detected through what is called a flux-locked loop (FLL) electronics system. The electrical output can then be transformed into a digital signal through optical cables. This output is usually displayed on a computer system connected to the MEG.

An important aspect of a MEG system is the magnetically shielded room (MSR). As mentioned, there are many sources of noise in the external environment. For example, many MEG systems are installed at locations in buildings near elevators and in urban centers (there may be additional large sources of external noise generated by nearby streetcars and subways). Magnetic shielding can be a very effective method to shield the MEG system from outside noise (16). There are different components of an MSR that provide different types of shielding: ferromagnetic shielding, eddy current shielding, and active shielding. Ferromagnetic shielding requires ferromagnetic metal, such as nickel, to protect against low-frequency noise (~0.1 Hz) from external magnetic fields (i.e., earth's magnetic field, elevator) that are extremely detrimental for MEG recordings (17). Eddy current shielding is required for higher frequency noise (e.g., 60 Hz line noise); a thick layer of a conducting metal such as aluminum can provide this type of shielding (12, 18). Active shielding can be added to the ferromagnetic and eddy current shielding when there is a large fluctuation of the direct current field in the environment (e.g., to shield noise from nearby subways) (19). Depending on the need, an MSR can be made thick or thin (typically 20 cm in total), but there are associated costs and practical constraints, including the extremely heavy weight of a thick MSR.

The Current Dipole

MEG studies use the signal acquired to understand brain activity. The conundrum, however, is that this process requires a reverse inference that has assumptions based on the current knowledge of physics and neurophysiology. To understand the fundamentals of how brain activity is captured by the MEG, there are a number of fundamental electromagnetism terminologies to understand. The current that is generated by the movement of ions due to neuronal activity in the brain is referred to as the primary current. In electrical systems, the net charge of a system must be balanced out. In the brain, the primary current can consist of the active and passive components, and the active transport of ions may create a charge imbalance that can drive the charge

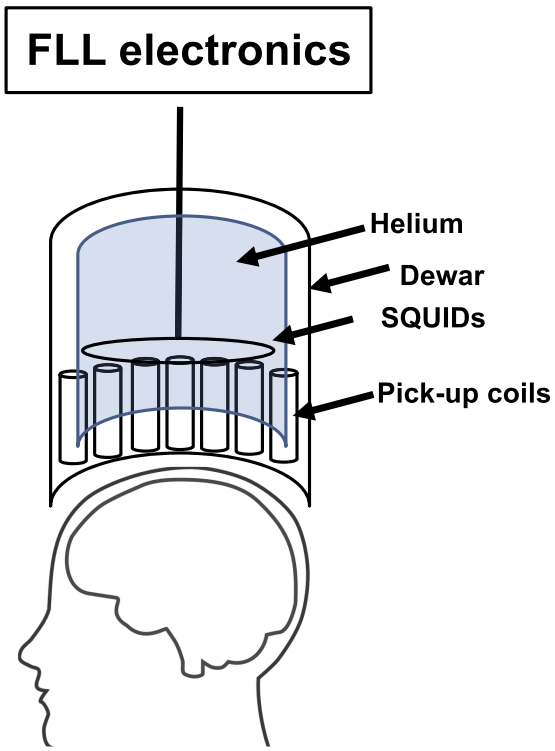

Figure 2. Circuit diagram of MEG instrumentation inside the MSR. FLL, flux-locked loop; MEG, magnetoencephalography; MSR, magnetically shielded room; SQUID, superconducting quantum interference device.

flow. The passive current, also known as the volume current, balances the charge imbalance via an extracellular current. These two currents generate the magnetic field that is measured by the MEG. The location of the neuronal activity can be approximated by what is known as the current dipole. Finally, the calculation of the magnetic field from the primary current and the local conductivity is called the forward problem (3).

Many of the approximations and assumptions involved in each step of the process of the forward problem is made possible through Maxwell's equations, the foundation of electromagnetism as we understand today. The first fundamental equation that describes the currents in the brain is the continuity equation (*Eq. 1*). This equation is required to calculate the electrical field and the magnetic field of a current (in this case neuronal activity) (3). The term ∇ is a vector operator used to indicate the divergence of the term J producing a scalar field, J denotes total current density, ρ denotes charge density, and t denotes time in *Eq. 1*:

$$\nabla \cdot J = -\frac{\partial \rho}{\partial t}. \quad (1)$$

To calculate the electric field of the current density, a "quasistatic" approximation is necessary. "Quasistatic" approximation refers to a condition where the propagation, conductance, and inductive effects can be ignored in a constant conductor (20) and as a result electric fields can be calculated as a scalar potential term (*Eq. 2*). This process greatly simplifies the necessary calculations for electric and magnetic fields. *Equation 2* is derived from the continuity equation and contains the term E representing the electrical field and the term V representing electrical potential as follows:

$$E = -\nabla V. \quad (2)$$

As mentioned, the currents in the brain can be divided into the primary current and the passive current. This current can be represented with *Eq. 3* (21, 22). In *Eq. 3*, the term J represents the current of the measured signal, J^P represents the primary current, and J^R represents the return current. *Equation 3* can then be simplified as *Eq. 4* by replacing the return current with the terms E for electric field intensity and σ for local conductivity as follows:

$$J = J^P + J^R; \quad (3)$$

$$J = J^P + E\sigma. \quad (4)$$

From the primary current at location $rJ^P(r')$, the current dipole can be calculated. In *Eq. 5*, the current dipole is represented by the term Q and the Dirac delta function (23) represented by the term δ. Both of these terms depend on current traveling from point A (r') to point B (r_0):

$$J^P(r') = Q\delta(r' - r_0). \quad (5)$$

The current dipole is crucial in MEG and electroencephalography (M/EEG) because the current dipole is thought to indicate the location of neuronal activity. Thus calculating the current dipole can be used to identify the location of the underlying neuronal activity from an indirect source such as the electrical potential of the EEG or the magnetic field of the MEG (24). The process of inferring source location based on measured magnetic field is known as the inverse problem in MEG. One problem of ambiguity with the current dipole is that it can be used to represent activity from a number of small areas that are part of the same region. An approach that can be used to simplify this issue is to use multipoles (25). Multipoles can be used to represent multipolar elements centered around a source, which is useful to represent a large area (26–28). A study which tested the effectiveness of the multipole model compared with the dipole model found that the multipole was superior in localizing the source compared with the single dipole (26). As such, the multipole provides a promising alternative to the traditional single dipole.

The Inverse Problem

Each inverse problem in MEG requires a unique solution (depending on the parameters such as shape of the conductor, distribution of current) to determine the location of the original signal. However, cases of the so-called "ill-posed" inverse problems (6) can arise when: *1*) there is no mathematical solution that can explain the source of the signal observed; *2*) the mathematical solution to the inverse problem is not unique (i.e., the signal can be localized to several different regions); and *3*) the mathematical solution to the inverse problem can vary greatly depending on small changes in parameters (e.g., current distribution) (29). In MEG, all three of these "ill-posed" problems may occur because: *1*) there may be noise present that prevents a solution from being determined; *2*) external magnetic field alone cannot be used to reconstruct an internal current [this phenomenon was first shown by Helmholtz (30)]; *3*) the data may change drastically depending on where the source is located (i.e., deep sources, sources far from the conductor) (14). These factors illustrate the difficulty in calculating current dipoles inside the head. One of the important caveats for MEG measurements is that radially oriented currents are mostly unable to be detected because the measured magnetic field from the primary current becomes zero when the dipole is oriented radially to the conductor model (e.g., in the case of the brain, the medial surface) in a perfectly spherical conductor model (31). EEG does not suffer from this problem because EEG measures the electrical field on the scalp from the primary and secondary current instead of the magnetic field outside of the head. The type of sources that are detected in MEG and EEG make them complementary techniques. There are several different types of localization techniques that may be used to solve the inverse problem. One approach is to use the least squares analysis to acquire the source estimates necessary for the localization of signal (32). In least squares analysis, the goal is to minimize the square of the difference between the predicted source model compared with the actual source model. Another well-established method to solve the inverse problem is to use minimum-norm estimates (MNE) (33, 34). MNE was designed to be able to calculate the electric or magnetic field at a given point in the brain, and it is a method that is used to find the shortest current vector that is able to explain the measured signals. Equivalent current dipole is another method for localization categorized under dipole methods where one or more dipoles are placed and moved around in the brain until the pattern of dipoles match the measured signal (35). The

equivalent current dipole method is the most popular method of source localization in the clinical setting, most often used to model interictal spikes. Finally, there are beamformers that are used and these will be discussed in depth in a latter section.

Forward Problem

The forward problem in MEG describes the process of calculating the magnetic and electrical field from neuronal sources. The magnetic field from a current is calculated using the Biot-Savart law (36) (see *Eq. 6*). In *Eq. 6*, the magnetic field term is B and it is dependent on the current represented by the term J obtained from *Eq. 4* once the return current can be calculated. The term r represents the position of the current and the field and the term d represents magnetic momentum. The term μ_0 is a constant term for vacuum permeability:

$$B(r) = \frac{\mu_0}{4\pi}\int J(r') \times \nabla' \frac{1}{r - r'} \mathrm{d}^3 r'. \quad (6)$$

For MEG, there are also magnetic fields measured outside of the head. For this calculation, the Biot-Savart law was modified as *Eq. 7* to calculate magnetic fields outside of the head (14, 31). In *Eq. 7*, the term p represents the current dipole and the term F is a term to represent change in the position of the current as denoted in *Eqs. 8* and *9*. The term r and r_0 represent positions at which magnetic fields can be calculated:

$$B(r) = \frac{\mu_0}{4\pi F^2}\left[F_p \times r_0 - (p \times r_0 \cdot r)\nabla F\right], \quad (7)$$

$$F = a(r \cdot a + ra), \quad (8)$$

$$a = r - r_0. \quad (9)$$

The Sarvas formula (31) calculates the magnetic field outside of the head generated by a current. The calculated magnetic field is independent of conductivity (i.e., the magnetic fields measured by the MEG). In addition, *Eq. 7* developed by Jukka Sarvas (31) can also explain why sources in the same radial direction as the original position of the current is silent to the MEG (only in a perfectly spherical conductor model) as $B(r)$ becomes 0 when $p \times r_0$ is equal to 0.

One element that needs to be considered for the inverse problem and forward modeling is the conductor (in this case the brain). Because it is not possible to measure the exact conductivity of the medium where the currents of interest pass through, models are used to approximate the brain as a conductor. Traditionally, the spherical head model was used for forward modeling (37). Although some studies have demonstrated that a sphere is a good approximation of the brain, the spherical model may be very inaccurate for localization of deep sources (38). Other studies have shown that the spherical model could be limited in exact localization (39). However, the sphere model still remains widely used and provides good localization for nondeep sources in the brain. Many researchers have investigated the effects of alternative head models for localization and found that these other more realistic models may be superior to the spherical model. However, model effects on localization are much more pronounced in EEG compared with MEG, and so this is a factor that contributes to the superiority of MEG compared with EEG with regards to spatial resolution (40).

The signal measured by MEG at any instant can be represented as neuronal activity by calculating the lead field. The lead field can be calculated from the magnetic field created by a specific current dipole when the local conductivity and geometry are assumed. The geometry of the volume conductor refers to the assumed shape of the conductor so that the forward calculation can be made. Thus, the volume conductor must be determined before the lead field can be calculated. Once calculated, the lead field is used in one of the last steps before processing the MEG signal to interpret neuronal activity from the brain. For application in MEG, an important property of the lead field arises from Helmholtz's reciprocity theorem where the lead field is the same as the electric field of a current in a conductor (41). This allows the location of the current dipole to be switched with the detector without affecting the measured amplitude of the signal. Lead field calculation is also extremely efficient compared with boundary element and finite element methods to solve the forward problem (42), thereby reducing the computing load for the forward calculations.

PRINCIPLES OF BEAMFORMING

Beamforming is currently one of the most common approaches to MEG source reconstruction. The idea of beamformers or beamforming was first developed for use in stationary radar systems. It was named for the "pencil beams" that were made to measure signals from a designated location while suppressing signal from other locations (43). The basic idea of beamforming is that signals from each sensor are filtered so that only the contributions from the signals of interest can be extracted through the sum of contributions from each sensor for the signal of interest. The spatial specificity of the beamformer comes from the fact that each distinct source has a unique sum of vector weightings (i.e., contribution of sensors) and thus are independent of each other (43). One way to think about beamformers is to imagine a mother who is able to locate their child's voice in a children's choir because in her brain she has the exact calculations that represents her child's voice and can thus isolate her child's voice among many others. The spatial specificity of the beamformer is instrumental to its application in MEG to locate exactly where in the brain signals from the sensors are coming from.

In beamforming, the covariance matrices are calculated from the source of interest at a time point from the measured magnetic field (44). In the most ideal case (i.e., a signal without source leakage) in beamforming, all of the covariance matrices arise from a single source location. In such a case, the equation described by Mosher et al. (254) is shown in *Eq. 10*, wherein C_j represents the source covariance matrix and C_b represents the data covariance matrix for given neuronal activity Q:

$$Q = C_j L^T C_b^{-1} B. \quad (10)$$

Covariance is a statistical term calculated from the sum of squares. If the covariance matrices are calculated from independent sources, the calculated power from this source will

be maximal whereas if there are many sources contributing, the power will be minimal. Because beamforming is calculated from the local lead field of neuronal activity, erroneous reconstruction of sources may occur quite frequently with close distance sources. This can be problematic when trying to analyze brain activity from regions that are close in proximity to each other and may especially be problematic for functional coupling (FCp) calculations.

Other than the localization issue, some additional shortcomings of the beamformer includes its dependency on the lead field. Any distortions or problems with the calculation of the lead field (e.g., the head model used, signal to noise of the scan) may have a large impact on the beamformer calculation. Another potential issue of the beamformer is that it focuses on regions of highest power. Thus, if the regions of interest are found within these high-power regions, the beamformer may not be sensitive enough to pick up the changes in power over time. As such, calculating the covariance matrices at a given time point in these high-power regions may not be accurate (44). For single source beamformers, one of the major disadvantages is that the beamformed power from spatially separate but temporally correlated sources can be suppressed (45). However, multisource beamformers can be used to overcome this problem.

Beamforming Techniques

Currently, there are many different types of beamforming techniques being used in the field of MEG. One of the earliest applications of beamforming in M/EEG was the method developed by Van Veen et al. (46) called the linearly constrained minimum variance (LCMV) beamformer. The LCMV was first developed for use in EEG and is used to calculate three separate spatial filters that make up the elements of the current dipole for each location of the brain at a given time point. The name "linearly constrained minimum variance" denotes that the goal of each spatial filter is to minimize the variance of the spatial filter outputs. When the outputs are calculated, the amount of variance from a location can be represented as the amount of activity that was measured in that location. The important caveat is that the beamformed sources are not necessarily due to activity from one source but may arise from a combination of dipoles. As such, LCMV also has the aforementioned shortcoming of beamforming when source localizing from two closely located sources leads to one calculated source. Nonetheless, the LCMV is an improvement on previous source localization methods because the number of active sources do not need to be defined before localization (46) (Table 1). In the other methods that required predefined active sources, any discrepancy between the previously defined sources and detected sources led to inaccurate locations for the reconstructed sources. Other vector beamformers (i.e., three-dimensional elements are used to reconstruct of sources) use a similar approach to the minimum variance beamformer in their approach (47, 48), although they differ on their mathematical approach to the beamforming problem (49).

Another early technique used for beamforming is the multiple-signal classification (MUSIC) algorithm (50, 51). MUSIC was first developed as a signal processing to locate the emitter from several antenna arrays (52). MUSIC is a time-frequency source estimation method where the volumetric dipoles are calculated for a location based on the signals measured over time. Due to the nature of the calculations, MUSIC assumes the dipole orientation from a source and thus is fundamentally different from a beamformer such as LCMV, which calculates spatial filters for a given time point (50, 51) (Table 1). This also means that MUSIC is not specifically designed to measure spontaneous activity. Another interesting assumption built into MUSIC is that MUSIC assumes that there are fewer sources than sensors distinguishing MUSIC from other beamformers.

The last of the widely used early beamformers is synthetic aperture magnetometry or SAM (47). SAM is a type of a minimum variance beamformer that differs from conventional beamformers as it is sensitive to voxel location and source orientation (47, 53). As such, SAM can be used in conjunction with structural MRI to provide higher spatial resolution compared with the other beamformer methods (54). One study that compared the beamformer methods of MUSIC, SAM, and LCMV found that SAM was superior to LCMV and comparable to MUSIC when reconstructing signals on simulated data for single dipoles (55). Another advantage of SAM (at the time of development) was that SAM introduced the idea of regularization to vector beamforming (56). Regularization

Table 1. *Characteristics of source localization techniques*

Source Localization Technique	Strengths	Weaknesses
LCMV	• Number of active sources do not need to be defined before localization • Improved source localization compared with other techniques that require predefined sources • Can measure instantaneous activity	• Source localizing from two closely located sources may lead to one calculated source • Beamformed sources do not necessarily reflect underlying activity
MUSIC algorithm	• Assumes fewer sources than sensors thus reducing rate of false positives	• Not designed to measure spontaneous activity • Assumes dipole orientations from a source
SAM	• Used in conjunction with MRI thus improving spatial resolution • Superior compared with LCMV and MUSIC for single dipoles • Introduced regularization (however now used by other vector beamformers) • Is suitable for transient events	• Requires structural MRI for source localization

LCMV, linearly constrained minimum variance; MUSIC, multiple-signal classification; SAM, synthetic aperture magnetometry.

refers to the compensatory process for increasing the signal-to-noise ratio for sources further away from the sensor (i.e., deep sources) by normalizing sensor noise at a particular voxel to all the other noise. As an alternative beamforming technique, several proof of concept studies confirmed the spatial acuity of SAM and showed that SAM could be used to reconstruct transient activations (57, 58) (Table 1). As such, SAM has been widely used for event-related beamforming since it was first introduced.

Other types of beamformers in use today also include dynamic imaging of coherent sources better known as DICS (59), which is used to calculate the power and coherence of reconstructed sources. There is also a new version of the minimum variance beamformer known as the multisource minimum variance beamformer (60). This version of the minimum variance beamformer is designed to deal with the high correlation issue in closely located sources. Through simulations, the authors demonstrated that the multisource minimum variance beamformer is indeed superior to single-source beamformers for correlated sources and that no prior knowledge of the sources are necessary for the reconstruction, thus it may be a vast improvement from the traditional vector beamformers especially for FCp analysis.

Overall, there are several beamforming techniques and many have become a staple in MEG research for source reconstruction. In an age of connectomics analysis, the development of atlas-guided beamforming (61) has further increased the usefulness of beamforming in MEG analysis. Thus, future developments similar to the multisource minimum variance beamformer may improve upon this widely used technique.

FUNCTIONAL COUPLING METHODS IN MEG

The concept of functional connectivity (FC) in functional MRI (fMRI) studies and FCp in MEG refers to mechanisms of how the brain works through functional segregation and integration (62). In the neuroimaging field, the term "functional connectivity" was first defined by Karl Friston as "the temporal correlations between spatially remote neurophysiological events" (63). There have been neurophysiology studies investigating the Hebbian idea of neuronal segregation that used multiunit recordings to investigate functional segregation of different neuronal populations (64, 65). These studies correlated multiple neuronal spikes from different regions and investigated the relationship between the firing patterns of neurons in different regions (66–69). The conclusion from the neurophysiological studies was that neurons from different regions have correlated spiking patterns and these correlations between brain regions can be modulated intrinsically and also by extrinsic (e.g., external stimulus) drive (64, 65). On a regional level, early neuroimaging studies used positron emission tomography (PET) and EEG to correlate neuronal activity between different brain regions. EEG studies examined the correlation between activity measured from different electrodes during a task (70–72). Early PET studies examined correlations of cerebral metabolism at "rest" between different brain regions (73–75). These PET studies were able to identify several regions of the brain that had correlated cerebral metabolism at rest. Later studies used PET and fMRI to measure FC during the so-called resting state or task-free functional neuroimaging of the brain (76, 77). This is what is now commonly known as resting-state FC based on the idea that in a task-free environment, the brain has a "default" mode or state (78) and that brain activity during these default resting-state time series can be correlated against each other in their baseline states (79). This line of analysis led to the discovery of the default mode network (DMN) (78, 79) and the discovery that during "rest" the brain actually consists of various sets of regions or functional networks that fluctuate in and out of correlation and anticorrelation (80, 81). Furthermore, there was more than just the DMN observed with resting-state FC such as networks involved in auditory, visual, and attention (82). These studies have been the foundation of many studies in neuroimaging that have used resting-state paradigms to investigate about brain mechanisms or abnormalities in disease models (83–86).

Phase Coupling

In M/EEG, the concept of FCp has been measured through the idea of coherence. The term coherence refers to the correlations between two different sources using their phase (87, 88) (Fig. 3*B*) (Table 2). Generally, coherence is used interchangeably with phase synchrony (91). As such, coherence is quantified as the amount of average phase synchrony over time (92, 93). In M/EEG, coherence may be different across different frequency bands. Thus, coherence in M/EEG can be used to interrogate functional band-specific integration and segregation of brain regions. However, coherence measures are not suitable for nonlinear, nonstationary data (94). As such, other approaches have been developed to study oscillatory organization for nonstationary systems. One of the oldest methods that was developed for this purpose is phase-locking value (PLV) (95). Determination of PLV involves calculating the instantaneous phase for two signals, computing the phase angle difference between the two signals, and then computing the consistency or stationarity of those phase angle differences. This measure provides a quantitative value of the phase synchrony between two signals of interest, and this provides insight into synchrony at given time point or an average of synchrony over a designated time period. As such, PLV can be used to investigate resting state synchrony between brain regions and has been used to investigate healthy and disease states (96–100).

Another method to quantify synchrony between two signals is synchronization likelihood (94). The concept of synchronization likelihood is that at a given time point, the measure describes how strongly a signal is synchronized to other signals where synchrony is determined by similarity of two signals. Since development, synchronization likelihood has been used to study disease states such as epilepsy and Alzheimer's disease (AD) (101, 102). The studies show promise for synchronization likelihood to detect differences between disease and healthy states. A measure that can be applied to resting-state recordings are useful for a disease such as epilepsy because it allows for measurement of synchrony during epileptic events and compare against silent periods (94, 103).

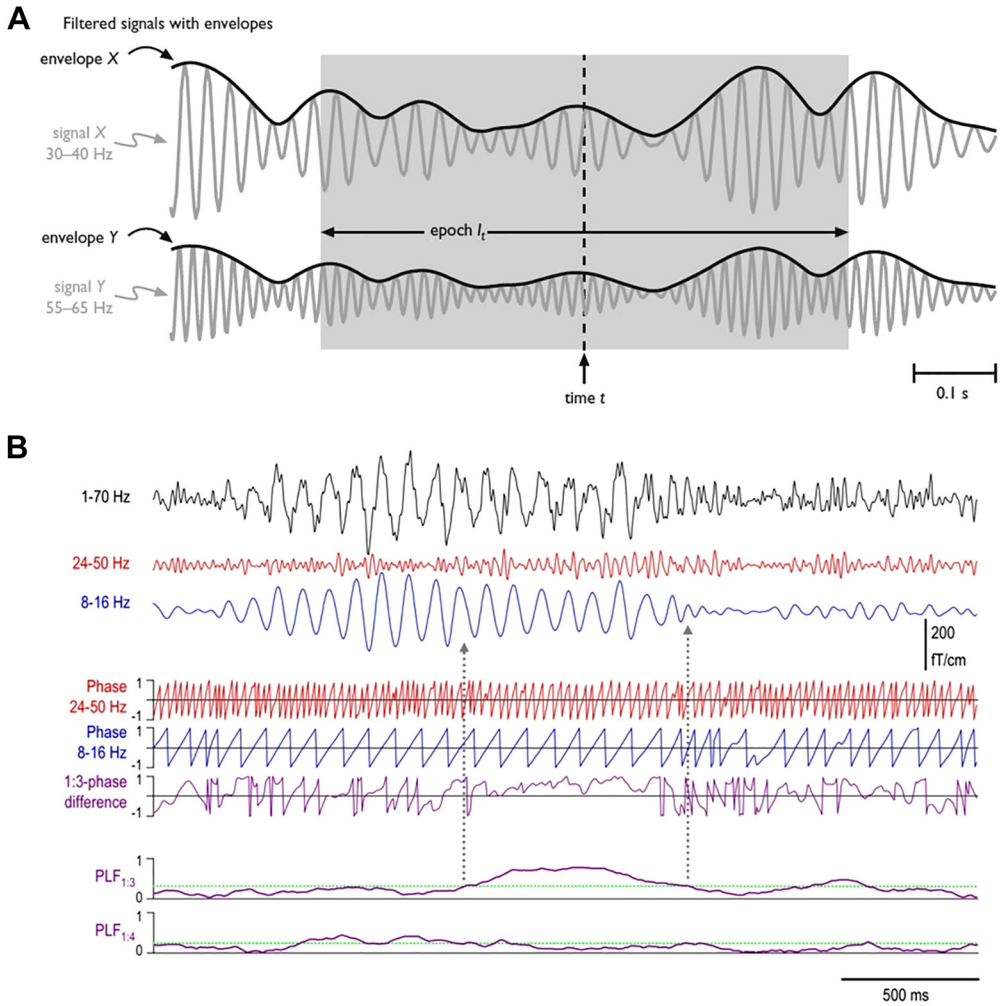

Table 2. *Characteristics of coupling metrics*

Coupling Category	Functional Coupling Measures	Associated Functional Properties
Amplitude coupling	• Amplitude-envelope correlation • Amplitude-amplitude correlation • Power-power correlation	• Long-range network level organization • Similar to fMRI resting-state networks • Robust metric that is associated with many brain functions
Phase coupling	• Phase coherence • Phase-locking value • Phase lag index	• Network-level functional brain organization • Short-range network level organization
Cross-frequency coupling	• Phase-amplitude coupling • Modulation index • Multilayer analysis	• Within- and cross-regional organization of different functional bands • Modulation of high-frequency oscillations by low frequencies (e.g., thalamocortical coupling, hippocampal coupling) • Predictive coding

fMRI, functional MRI.

Among phase synchrony/coupling measures being used, one of the most widely used measures has been the phase lag index (PLI) (104) and the variations such as the weighted phase lag index (wPLI) (105) and the directed phase lag index (106). The PLI is a mathematical calculation between two signals where nonzero phase lag between two signals are calculated and summarized as an index value where 1 represents maximal phase synchrony and 0 represents no synchrony. A study of PLI demonstrated that PLI performs equal or better than phase coherence or imaginary coherence to measure synchrony across the brain (104, 107). Thus, there is promise that this measure might be the best measure to quantify phase synchrony. Several studies have examined PLI in both healthy and disease states (108–113) and showed that it was a meaningful measure to capture large-scale organization in the human brain. There are some disadvantages to using PLI, namely, the PLI's sensitivity to volume conduction and sudden changes in phase (i.e., a sudden change in instantaneous phase from phase lag to a phase lead). As such, an improved measure known as the wPLI was developed where the PLI is weighted by the imaginary component of the cross-spectra (105). The comparison analyses between the imaginary coherence, PLI, and wPLI showed that the wPLI was best at controlling for false positives associated with volume conduction. The wPLI was also the best method to detect nonzero lag phase synchrony. Therefore, wPLI serves as an improved alternative of the PLI for FCp analyses.

Amplitude Envelope Correlation

Another popular FCp technique that is different from the phase coherence measures is known as amplitude envelope correlation (AEC) (89) (Fig. 3*A*) (Table 2). Amplitude envelope correlation involves calculation of the spectral amplitude envelope from a time series using a Fourier transform, and then the correlation between the two envelopes is calculated within a given time window. The bandpass-filtered version of the AEC utilizing the Hilbert transform (114, 115) was used in latter studies to investigate band-to-band AEC between brain regions. Another implementation to the AEC technique is orthogonalization (116–118). As with many of the FCp metrics, source leakage leading to false coupling is a serious issue in MEG. As such, the process of orthogonalization tries to combat this problem by removing correlations with zero phase lag and by removing the linear dependencies from two signals, which lead to two signals being orthogonal to one another (hence the term orthogonalization). Applying orthogonalization was shown to correct for source leakage issues thus being advantageous for MEG FCp research, especially with sources close to one another (114, 117). Thus, orthogonalized AEC is a method that can be used to study functional integration and segregation of the brain while limiting source leakage in MEG. In addition, the AEC is an MEG FCp measure that best reflects the resting-state networks from the blood oxygen level-dependent (BOLD) fMRI signal (114, 119).

Cross-Frequency and Phase-Amplitude Coupling

Cross-frequency coupling (CFC) is a technique used to probe brain function. CFC refers to phase-phase, amplitude-amplitude, phase-amplitude, phase-frequency, amplitude-frequency, and frequency-frequency couplings that occur across different frequencies (Fig. 3*C*) (Table 2) (90, 120–123). Among the variation of CFC, phase-amplitude coupling (PAC) is the most frequently used technique. CFC and PAC have been most extensively used in studies of cognition and memory. An example of PAC includes the seminal work showing θ-γ coupling within a single brain region (e.g., hippocampus, prefrontal cortex) associated with functions such as encoding and working memory (124–127). This pattern of a low-frequency to high-frequency coupling is thought to

Figure 3. Concept of amplitude and phase-based coupling. *A*: amplitude-envelope coupling is demonstrated where the calculated envelopes between two time series are correlated over a designated period of time. Adapted from Bruns et al. (89) with permission. *B*: phase coupling is demonstrated between two time series with different phases. Phase synchrony between the time series are marked by the gray arrows. Adapted from Palva et al. (88) with permission. Copyright 2005 Society for Neuroscience. *C*: different types of cross-frequency coupling (CFC) observed, including phase-amplitude coupling. *a*: a low-frequency signal that has a fluctuating amplitude. *b*: amplitude-amplitude coupling: high-frequency signal's amplitude (Y1) is modulated by the low-frequency signal's amplitude (X). *c*: phase-phase coupling: signals X and Y2 have a 3:1 phase relationship, where one oscillation of X is coupled with three oscillations of Y2. *d*: phase-amplitude coupling: amplitudes of the signal Y3 is coupled with the phase of signal X. *e*: phase-frequency coupling: frequency modulations in signal Y4 is coupled to the phase of signal X. *f*: amplitude-frequency coupling: frequency modulation in signal Y5 is coupled to the amplitude of signal X. *g*: frequency-frequency coupling: differences in frequency modulations are seen in signal Y5 and Y6. Adapted from Jirsa and Müller (90) with permission.

involve phase of the low frequency oscillation actively modulating the amplitude of high-frequency oscillations through PAC mechanism (128). This phenomenon had first been observed in electrophysiology studies in the rat hippocampus (129, 130). Current studies have also used PAC to study disease states such as Parkinson's disease to measure the impact of the disease as well as therapeutic effects (131, 132). Interestingly, a study demonstrated that PAC was ubiquitous across the brain and that resting-state networks (RSN) also exhibited PAC (133). Thus, future research in healthy and diseased states that focus on cross-regional cross-frequency modulation is important to examine the multifaceted and complex organization of brain function.

Methodological Considerations with Functional Coupling Methods

Techniques to measure FCp provide an opportunity to examine intrinsic brain networks. However, many factors can impact measures of FCp, and so it is important to determine the reliability and accuracy of FCp measures in MEG compared with ground truth. Some factors that may affect the accuracy and reliability of FCp in MEG include: connectivity between sensors or sources that share signal contribution from the same regions (i.e., source leakage) (116, 117, 134), limited spatial resolution of the MEG, and low signal-to-noise ratio compared with fMRI (135).

There are only a couple of studies that examined the impact of MEG limitations on measures of FCp. One study found that using MEG, sensor space FCp graph analysis metric reliability was dependent on whether the subject had their eyes open or closed during the resting-state scan (136). This study also demonstrated that the reliability of FCp graph analysis metrics depends on the type of measure used and the functional band. It was observed that γ-band FCp graph analysis metrics had poor reliability and α/β bands had the highest reliability (136). There was also a difference between the eye-open and eye-closed conditions and the greatest difference was observed in the α band. Another study investigated the reliability issue using a region of interest (ROI) based approach with many of the metrics used in the literature such as AEC, coherence, PLV, PLI, and other metrics (135) (Fig. 4). The results confirmed findings from a sensor level study that α-band FCp graph analysis metrics was most consistent between the different measures in group level comparisons (137). It was also observed that FCp measures which did not correct for signal leakage (i.e., through orthogonalization or through zero lag metrics) had better consistency in the group-level inference of different networks (135). Finally, both within- and between-subject consistency of networks across different sessions was highest in metrics which did not have leakage correction (135). It was postulated that in the metrics without leakage correction, there was a lot of spurious coupling and shared signals that led to an inflation of the reliability metrics. These results indicated that there may be a large contribution of spatial leakage into FCp metrics in MEG if they are not accounted for. However, orthogonalized AEC showed comparable reliability to uncorrected FCp measures, demonstrating that orthogonalized AEC could act as a reliable, leakage-free method. A more recent study used FCp graph analysis measures to assess the reliability of static and dynamic FCp metrics (138). This analysis demonstrated that static functional graphs were more reliable with correlation compared with imaginary PLV. Imaginary PLV refers to a PLV measure built on the concept of imaginary coherency thus providing a measure free from effects of signal leakage (139). However, the dynamic functional graph demonstrated much improved reliability in both correlations and with imaginary PLV. This suggested that dynamic but not static measures of FCp was reliable between sessions at a group level in MEG.

Signal leakage in MEG FCp research are caveats that need to be carefully considered, and thus different groups have investigated the presence of artifactual coupling and spurious coupling using different metrics for FCp. Artifact coupling refers to false positive due to signal spread in MEG source reconstruction whereas spurious coupling refers to false-positive coupling due to signal leakage from two sources which have significant "ghost" interactions (140). "Ghost" interactions refer to false-positive interactions that reflect true interactions with misestimated locations. A simulation study found that even the methods designed to combat artifact coupling (i.e., orthogonalized AEC, wPLI) are prone to having false-positive coupling results due to spurious coupling (140). Furthermore, the presence of signal leakage was found to cause different degrees of artifact coupling and spurious coupling in each coupling metric, with the coupling measures not accounting for signal leakage, showing much higher levels of spurious coupling whereas coupling measures accounting for signal leakage showing lesser amounts of true coupling. Thus, false coupling is inevitable due to the limitations of source reconstruction methods even with FCp methods designed to combat signal leakage. One method proposed to account for false coupling is hyperedge bundling (141). This technique used a graph approach to form edges between two sources and hyperedges were formed by combining similar edges that may include true and spurious interactions. Through this process it was observed that although there are still a number of spurious interactions, there is a reduced occurrence of spurious interactions compared with other methods of correcting for signal leakage (141). As such, this technique can limit the ratio of spurious coupling, but it will not correct for them entirely. In addition to source leakage, there may be discrepancies in the FCp metrics obtained due to differences in the hardware. Differences in the RSNs derived from MEGIN (formerly known as Neuromag) and CTF machines were observed. Neuromag machines can show increased number of deep-source FCp compared with CTF machines, and this result may or may not be a false positive (K. Singh, unpublished observations). One possible reason for this discrepancy may come from the fact that the CTF and the MEGIN systems employ different types of sensors. Several studies investigating the discrepancy in the measured signal between the systems have reported some variability in the measured signal between the two systems (142–144). In particular, the most recent study demonstrated that there was ~8-mm variability between the two systems in localizing the primary somatosensory cortex (143). The caveat is that the studies investigating the discrepancies observed evoked signals while the reported discrepancy was present in resting-state networks. Furthermore, the published studies did not investigate

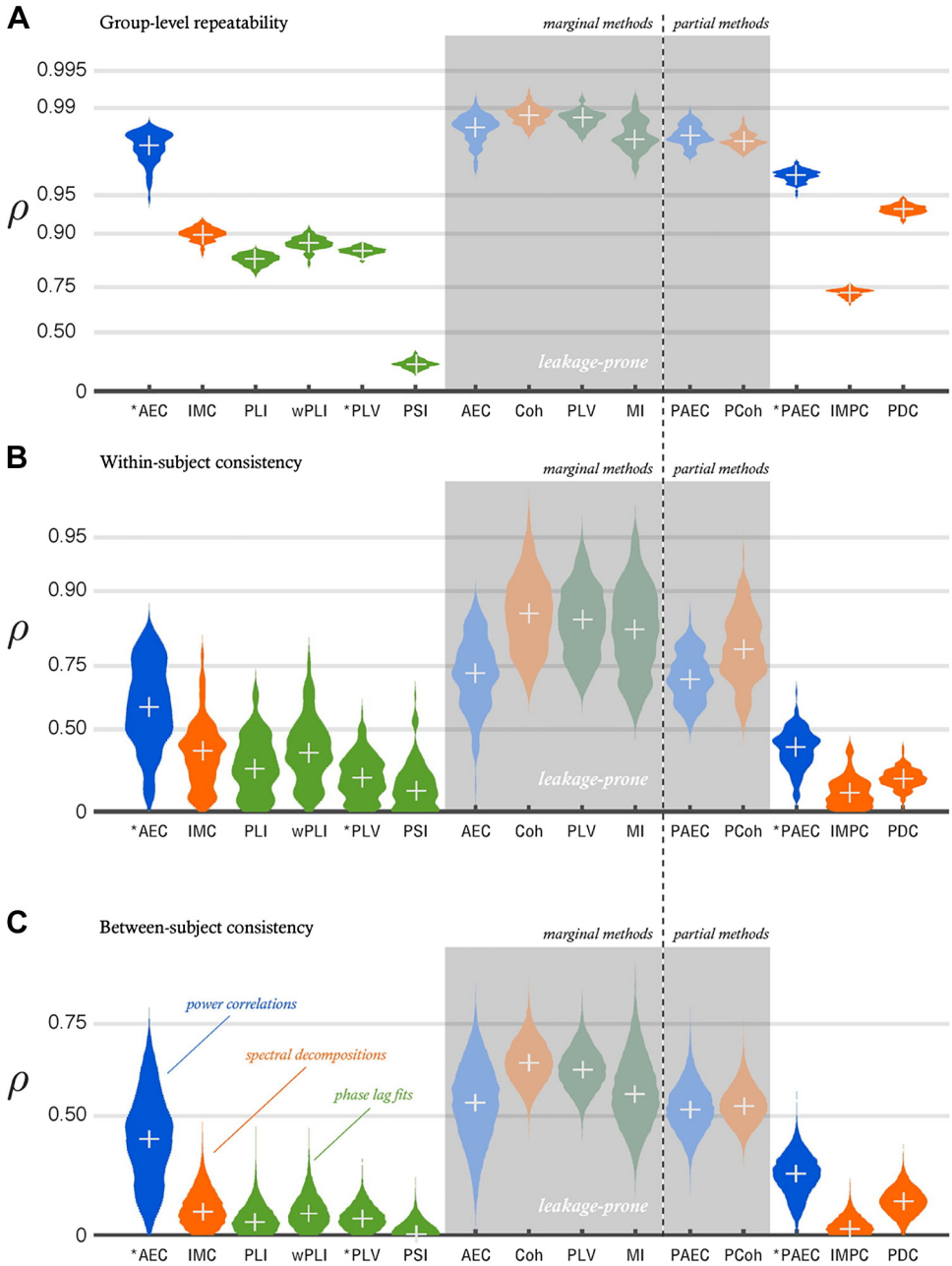

Figure 4. Consistency of different functional coupling (FCp) metrics. Group level reliability (*A*), within-subject reliability (*B*), and between-subject reliability (*C*). AEC, amplitude envelope correlation; Coh, band-averaged coherence; IMC, band-averaged imaginary component of coherency; IMPC, partial imaginary coherence; MI, mutual information of phases; PAEC, partial amplitude envelope partial correlation; PCoh, partial coherence; PDC, partial directed coherence; PLI, phase lag index; PLV, phase locking value; PSI, phase slope index; wPLI, weighted phase lag index. Adapted from Colclough et al. (135) with permission.

signals from deeper sources. Thus, there may be unknown discrepancies between the two MEG systems that may need to be identified especially for resting-state studies.

CURRENT AND POTENTIAL USE OF MEG IN CLINICAL POPULATIONS

Currently, the most popular clinical application of MEG is for epilepsy (145). For example, MEG can be used to monitor ictal activity, providing a better spatial localization compared with EEG (146–148). The use of MEG in presurgical monitoring of interictal activity has greatly improved surgical outcomes (149–153). Furthermore, MEG has been used to determine the lateralization and localization of language in presurgical epilepsy cases (154–157). With the development of improved FCp methods, many studies have investigated altered FCp in epileptic patients (158–160). These studies identified lateralized FCp abnormalities that could be used as potential markers for clinical decision-making. In addition, improvements in source localization techniques (i.e., improved accuracy for localization of signal, ability to pinpoint more accurate focal regions) have led to an improvement in the surgical outcomes for epilepsy (161–166) (Fig. 5*A*). These studies have shown that source imaging with MEG or combined EEG-MEG is as effective as MRI and invasive recordings for locating affected brain regions.

MEG studies of clinical outcomes in stroke have reported signs of recovery post stroke. MEG for clinical use in stroke

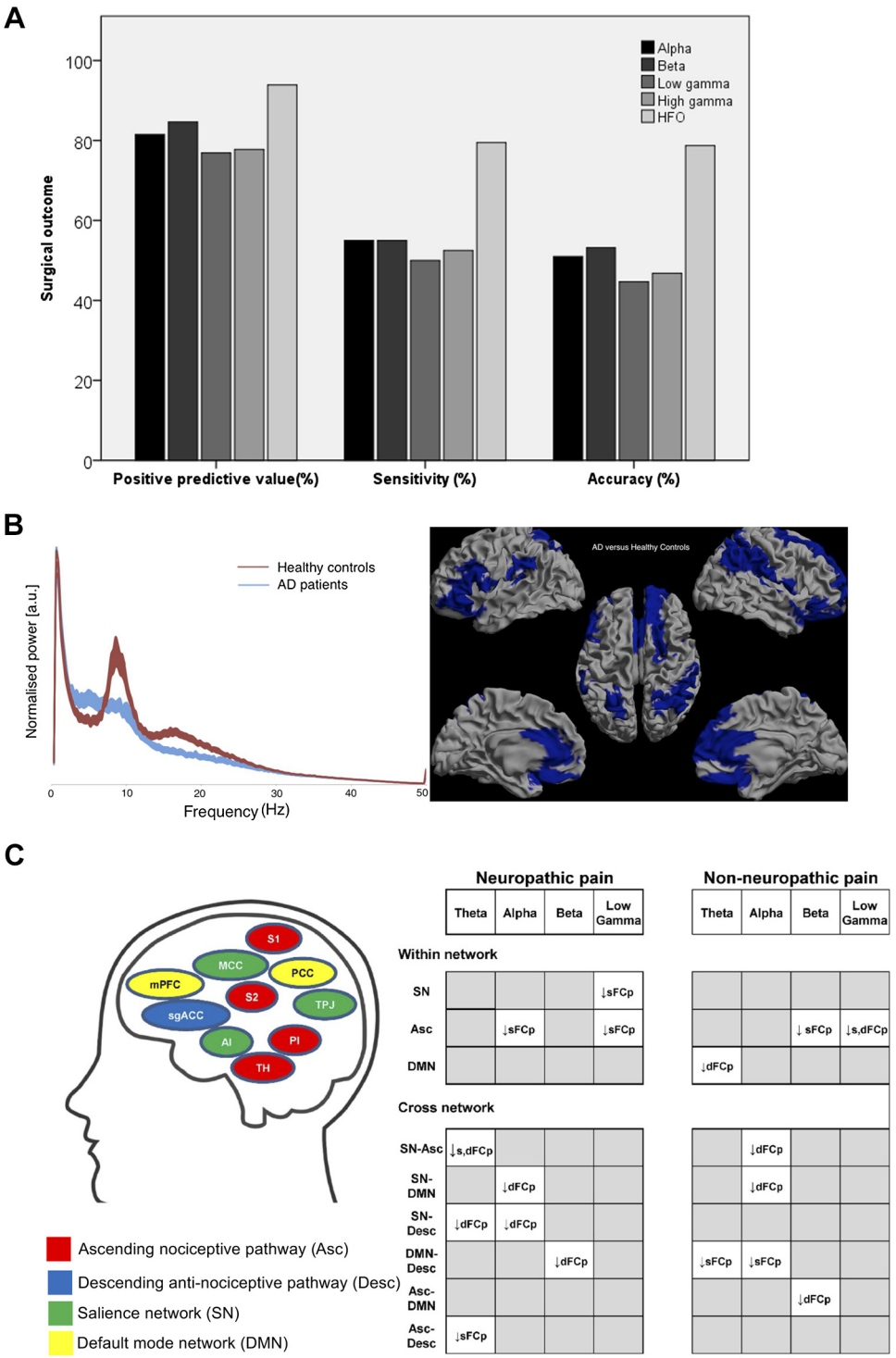

Figure 5. Examples of clinical applications of MEG. *A*: a study on epilepsy shows the sensitivity, positive predictive value, accuracy of surgical treatment based on activity from each frequency band in the epileptic zone. Adapted from Velmurugan et al. (166) with permission. *B*: a study on Alzheimer's disease shows global peak frequency slowing as a possible biomarker for Alzheimer's disease. Adapted from Engels et al. (167) with permission. *C*: a study on chronic pain shows widespread abnormalities of cross-network FCp. The FCp abnormalities are different based on the type of pain experienced by the people living with chronic pain. Adapted from Kim et al. (168) with permission. AD, Alzheimer's disease; MEG, magnetoencephalography.

has been proposed because magnetic fields do not change near necrotic tissue (169). Whereas MRI is severely impacted by altered hemodynamics. As such, many MEG studies of stroke have observed changes in the power spectra associated with post stroke recovery (170–172). In these studies, there was a broadband change in the spectral profile and the location of the power spectra changes was also variable. Other MEG studies observed spectral power and coherence changes in the motor cortex and correlated it to recovery of motor function (173–180). These studies demonstrated that MEG can be used as a possible marker for recovery of motor function in stroke. MEG studies have also investigated the neural correlates associated with the recovery of speech (181, 182) and found that recovery of function as measured by performance on language tasks was reflected by increased activity in the left hemisphere.

MEG has also been proposed as a neuroimaging method to detect traumatic brain injury (TB1) that does not have visible structural abnormalities (183). Thus, current MEG research has explored possible biomarkers of TB1 (184–194). Several abnormalities were noted from these studies, including increased γ power, abnormal resting-state cross-frequency coupling, and abnormal resting FCp mainly in the θ, α, and β bands. In addition, a study demonstrated that transcranial electrical stimulation is able to ameliorate some of the low-frequency power abnormalities in mild TB1 (195). As such, MEG may be a useful clinical technique to detect mild TB1, and, additionally, it could also serve as a marker to measure the efficacy of therapies for mild TB1.

MEG may also have utility for examining psychiatric disorders. For example, MEG is being used to investigate biomarkers of depression to predict depression severity (196, 197). Several studies of depression have detected brain abnormalities using MEG, in particular network-level abnormalities in the prefrontal regions and the limbic network (198–202) and the change in brain metrics associated with effects of treatment in depression (203, 204). Numerous MEG studies of other psychiatric conditions, such as schizophrenia (205–210), have demonstrated both network-level and regional power abnormalities in schizophrenia. In particular, schizophrenia has been associated with abnormalities observed in the DMN, the salience network, and the central executive networks as well as the visual and motor regions (211). One study in particular demonstrated the potential clinical use of MEG for schizophrenia by classifying an individual as schizophrenic through machine learning methods using dynamic FCp (212).

Another psychiatric disorder where MEG has been used widely is autism spectrum disorders (ASDs) (83, 213–218). It has been suggested that ASD is associated with reduced long-range FCp and decreased power in the low-frequency bands in resting-state studies (219). MEG has also revealed brain activity that was associated with abnormal auditory, visual, and emotional processing in ASD (220). Due to the wide range of brain metrics that can be measured by MEG, it has been suggested that MEG could be used for biological stratification of the different subtypes in ASD. Several MEG studies have shown alterations in brain activity associated Alzheimer's disease (AD) (103, 167, 221–226) (Fig. 5*B*). These studies demonstrated that MEG measures of brain abnormalities are related to severity of AD such as reduced cognitive function and the level of amyloid. Promising research for the clinical use of MEG in AD has identified several features associated with early onset AD, including widespread slowing of peak frequency in the hippocampus (167), slowing of peak α frequency (227), reduced signal complexity (228), and increased δ, θ, and α power associated with not only AD but also early cognitive decline (229). Other studies have employed multiple machine learning methodologies to identify features associated with mild cognitive impairment and early stage AD (230, 231), showing promise for MEG as a sensitive detection technique for early onset AD.

In the pain field, MEG has been used to measure brain abnormalities in several chronic pain conditions including: complex regional pain syndrome (232–234), fibromyalgia (235–238), migraine (239–241), neuropathic pain (168, 242, 243) (Fig. 5*C*), and menstrual pain (244, 245). Many studies have reported specific abnormalities pertaining to each chronic pain condition. However, there may be a common brain abnormality across different chronic pain conditions that can be identified using MEG (145). In particular, we and others have observed slowing of peak α frequency as a possible marker of pain sensitivity as well as neuropathic pain (242, 243, 246–248). There has also been an MEG study that tried to predict pain levels from resting-state MEG (244). However, the use of brain data to decide whether someone is in pain or whether an individual suffers from chronic pain is fraught with technical, scientific, biological, and ethical problems (249, 250). In addition to chronic pain, there may be ethical problems associated with using brain data to decide if an individual suffers from psychiatric disorders (e.g., depression, schizophrenia) as the symptoms are also not always visible in these disorders. As such, clinical use of MEG in pain and other diseases should focus on identifying brain features associated with effective personalized treatment and to identify brain features that allow for better characterization or stratification of complex disorders.

CONCLUSIONS AND FUTURE DIRECTIONS

MEG is an electrophysiological/neuroimaging approach that has utility in both basic neuroscientific explorations and clinical applications. There have been a number of other diseases where MEG metrics, such as FCp and power, have been observed to be a possible biomarker for treatment efficacy, disease severity, and disease stratification. In the near future, the advent of optically pumped magnetometers (OPMs) or the wearable MEGs (251) will allow MEG systems to be more accessible due to the lower cost and simplicity of the system that does not require SQUIDs. The OPMs use circularly polarized laser beams to optically pump alkali metal atoms, and the polarized atoms have a specific spin direction (252). However, the oriented spin direction can be changed with a magnetic field and a second light can be used to probe the change in spin orientation, and this process is used to infer information about the external magnetic field. Recent OPM MEG systems have been developed as multichannel, on-scalp MEG systems that allow the measurements to be closer to the brain and have similar spatial resolution compared with the SQUID systems (251, 253). As such, OPMs could potentially open an infinite amount of new applications for MEGs in clinical settings as hospital will not require MSRs to record MEG scans. As such, laying the foundation for future clinical application using the current MEG systems will be crucial, and further development in FCp techniques, source analysis techniques, and machine learning applications will all play an important part in this process.

ACKNOWLEDGMENTS

The authors would like to acknowledge Dr. Ben Dunkley for providing feedback on earlier versions of this manuscript.

GRANTS

This work was funded by the Canadian Chronic Pain Network, through the Strategy for Patient Oriented Research (Canadian Institutes of Health Research SCA-145102), the Canadian Institutes of Health Research (PJT 162347), and the Mayday Fund. J. A. Kim

was supported by an MS Society of Canada endMS Doctoral Studentship Award.

DISCLOSURES

No conflicts of interest, financial or otherwise, are declared by the authors.

AUTHOR CONTRIBUTIONS

J.A.K. conceived and designed research; J.A.K. performed experiments; J.A.K. analyzed data; J.A.K. interpreted results of experiments; J.A.K. prepared figures; J.A.K. drafted manuscript; J.A.K. and K.D.D. edited and revised manuscript; J.A.K. and K.D.D. approved final version of manuscript.

REFERENCES

1. **Oersted HC.** Experiments on the effect of a current of electricity on the magnetic needle. *Ann Philos* 16: 273–276, 1820. doi:10.1515/9781400864850.417.
2. **Fedele T**, **Scheer H**, **Burghoff M**, **Curio G**, **Körber R.** Ultra-low-noise EEG/MEG systems enable bimodal non-invasive detection of spike-like human somatosensory evoked responses at 1 kHz. *Physiol Meas* 36: 357–368, 2015. doi:10.1088/0967-3334/36/2/357.
3. **Hämäläinen M**, **Hari R**, **Ilmoniemi RJ**, **Knuutila J**, **Lounasmaa OV.** Magnetoencephalography—theory, instrumentation, and applications to noninvasive studies of the working human brain. *Rev Mod Phys* 65: 413–497, 1993. doi:10.1103/RevModPhys.65.413.
4. **Murakami S**, **Okada Y.** Contributions of principal neocortical neurons to magnetoencephalography and electroencephalography signals. *J Physiol* 575: 925–936, 2006. doi:10.1113/jphysiol.2006.105379.
5. **Okada YC**, **Wu J**, **Kyuhou S.** Genesis of MEG signals in a mammalian CNS structure. *Electroencephalogr Clin Neurophysiol* 103: 474–485, 1997. doi:10.1016/S0013-4694(97)00043-6.
6. **Nashed M.** Operator-theoretic and computational approaches to ill-posed problems with applications to antenna theory. *IEEE Trans Antennas Propagat* 29: 220–231, 1981. doi:10.1109/TAP.1981.1142564.
7. **Hillebrand A**, **Barnes G.** A quantitative assessment of the sensitivity of whole-head MEG to activity in the adult human cortex. *NeuroImage* 16: 638–650, 2002. doi:10.1006/nimg.2002.1102.
8. **Ahlfors SP**, **Han J**, **Belliveau JW**, **Hämäläinen MS.** Sensitivity of MEG and EEG to source orientation. *Brain Topogr* 23: 227–232, 2010. doi:10.1007/s10548-010-0154-x.
9. **Muthukumaraswamy S.** High-frequency brain activity and muscle artifacts in MEG/EEG: a review and recommendations. *Front Hum Neurosci* 7: 138, 2013. doi:10.3389/fnhum.2013.00138.
10. **Ahonen A**, **Hamalainen M**, **Kajola M**, **Knuutila J**, **Lounasmaa O**, **Simola J**, **Tesche C**, **Vilkman V.** Multichannel SQUID systems for brain research. *IEEE Trans Magn* 27: 2786–2792, 1991. doi:10.1109/20.133789.
11. **Ahonen AI**, **Hämäläinen M**, **Kajola M**, **Knuutila J**, **Laine P**, **Lounasmaa O**, **Parkkonen L**, **Simola J**, **Tesche C.** 122-channel SQUID instrument for investigating the magnetic signals from the human brain. *Phys Scr* T49A: 198–205, 1993. doi:10.1088/0031-8949/1993/T49A/033.
12. **Zimmerman JE.** SQUID instruments and shielding for low-level magnetic measurements. *J Appl Phys* 48: 702–710, 1977. doi:10.1063/1.323659.
13. **Clarke J.** SQUIDs. *Sci Am* 271: 46–53, 1994. doi:10.1038/scientificamerican0894-46.
14. **Supek S**, **Aine CJ** (Editors)**.** *Magnetoencephalography: From Signals to Dynamic Cortical Networks*. Berlin, Germany: Springer, 2014.
15. **Vrba J**, **Robinson S.** SQUID sensor array configurations for magnetoencephalography applications. *Supercond Sci Technol* 15: R51–R89, 2002. doi:10.1088/0953-2048/15/9/201.
16. **Cohen D**, **Schläpfer U**, **Ahlfors S**, **Hämäläinen M**, **Halgren E.** New six-layer magnetically-shielded room for MEG. *Proceedings of the 13th International Conference on Biomagnetism Jena*. Berlin, Germany: VDE Verlag, 2002.
17. **Cohen D.** Enhancement of ferromagnetic shielding against low-frequency magnetic fields. *Appl Phys Lett* 10: 67–69, 1967. doi:10.1063/1.1754854.
18. **Malmivuo J**, **Lekkala J**, **Kontro P**, **Suomaa L**, **Vihinen H.** Improvement of the properties of an eddy current magnetic shield with active compensation. *J Phys E* 20: 151–164, 1987. doi:10.1088/0022-3735/20/2/007.
19. **Platzek D**, **Nowak H**, **Giessler F**, **Röther J**, **Eiselt M.** Active shielding to reduce low frequency disturbances in direct current near biomagnetic measurements. *Rev Sci Instrum* 70: 2465–2470, 1999. doi:10.1063/1.1149779.
20. **Plonsey R**, **Heppner DB.** Considerations of quasi-stationarity in electrophysiological systems. *Bull Math Biophys* 29: 657–664, 1967. doi:10.1007/BF02476917.
21. **Barnard A**, **Duck I**, **Lynn MS.** The application of electromagnetic theory to electrocardiology: I. Derivation of the integral equations. *Biophys J* 7: 443–462, 1967. doi:10.1016/S0006-3495(67)86598-6.
22. **Geselowitz DB.** On bioelectric potentials in an inhomogeneous volume conductor. *Biophys J* 7: 1–11, 1967. doi:10.1016/S0006-3495(67)86571-8.
23. **Dirac PAM.** *The Principles of Quantum Mechanics*. Oxford, UK: Oxford University Press, 1981, p. 328.
24. **Schneider MR.** A multistage process for computing virtual dipolar sources of EEG discharges from surface information. *IEEE Trans Biomed Eng* 19: 1–12, 1972. doi:10.1109/tbme.1972.324152.
25. **Baillet S**, **Mosher JC**, **Leahy RM.** Electromagnetic brain mapping. *IEEE Signal Process Mag* 18: 14–30, 2001. doi:10.1109/79.962275.
26. **Jerbi K**, **Baillet S**, **Mosher J**, **Nolte G**, **Garnero L**, **Leahy R.** Localization of realistic cortical activity in MEG using current multipoles. *NeuroImage* 22: 779–793, 2004. doi:10.1016/j.neuroimage.2004.02.010.
27. **Nenonen J**, **Katila T**, **Leinio M**, **Montonen J**, **Makijarvi M**, **Siltanen P.** Magnetocardiographic functional localization using current multipole models. *IEEE Trans Biomed Eng* 38: 648–657, 1991. doi:10.1109/10.83564.
28. **Nolte G**, **Curio G.** Current multipole expansion to estimate lateral extent of neuronal activity: a theoretical analysis. *IEEE Trans Biomed Eng* 47: 1347–1355, 2000. doi:10.1109/10.871408.
29. **Weber CF.** Analysis and solution of the ill-posed inverse heat conduction problem. *I J Heat Mass Transf* 24: 1783–1792, 1981. doi:10.1016/0017-9310(81)90144-7.
30. **Helmholtz HV.** [Ueber einige Gesetze der Vertheilung elektrischer Ströme in körperlichen Leitern, mit Anwendung auf die thierisch-elektrischen Versuche (Schluss)]. *Ann Phys Chem* 165: 353–377, 1853. doi:10.1002/andp.18531650702.
31. **Sarvas J.** Basic mathematical and electromagnetic concepts of the biomagnetic inverse problem. *Phys Med Biol* 32: 11–22, 1987. doi:10.1088/0031-9155/32/1/004.
32. **Huizenga HM**, **Molenaar PC.** Ordinary least squares dipole localization is influenced by the reference. *Electroencephalogr Clin Neurophysiol* 99: 562–567, 1996. doi:10.1016/S0013-4694(96)95659-X.
33. **Hämäläinen MS**, **Ilmoniemi RJ.** Interpreting magnetic fields of the brain: minimum norm estimates. *Med Biol Eng Comput* 32: 35–42, 1994.
34. **Hauk O.** Keep it simple: a case for using classical minimum norm estimation in the analysis of EEG and MEG data. *NeuroImage* 21: 1612–1621, 2004. doi:10.1016/j.neuroimage.2003.12.018.
35. **Tenney JR**, **Fujiwara H**, **Rose DF.** The value of source localization for clinical magnetoencephalography: beyond the equivalent current dipole. *J Clin Neurophysiol* 37: 537–544, 2020. doi:10.1097/WNP.0000000000000487.
36. **Jackson JD.** *Classical Electrodynamics*. New York: John Wiley and Sons, 2007, p. 832.
37. **Huang M-X**, **Mosher JC**, **Leahy R.** A sensor-weighted overlapping-sphere head model and exhaustive head model comparison for MEG. *Phys Med Biol* 44: 423–440, 1999. doi:10.1088/0031-9155/44/2/010.
38. **Cuffin BN.** Effects of head shape on EEGs and MEGs. *IEEE Trans Biomed Eng* 37: 44–52, 1990. doi:10.1109/10.43614.
39. **Cuffin BN**, **Schomer DL**, **Ives JR**, **Blume H.** Experimental tests of EEG source localization accuracy in spherical head models. *Clin Neurophysiol* 112: 46–51, 2001. doi:10.1016/S1388-2457(00)00488-0.

40. **Cohen D**, **Cuffin BN**, **Yunokuchi K**, **Maniewski R**, **Purcell C**, **Cosgrove GR**, **Ives J**, **Kennedy JG**, **Schomer DL.** MEG versus EEG localization test using implanted sources in the human brain. *Ann Neurol* 28: 811–817, 1990. doi:10.1002/ana.410280613.
41. **Malmivuo J**, **Plonsey R.** *Bioelectromagnetism: Principles and Applications of Bioelectric and Biomagnetic Fields*. New York: Oxford University Press, 1995.
42. **Wolters CH**, **Grasedyck L**, **Hackbusch W.** Efficient computation of lead field bases and influence matrix for the FEM-based EEG and MEG inverse problem. *Inverse Problems* 20: 1099–1116, 2004. doi:10.1088/0266-5611/20/4/007.
43. **Van Veen BD**, **Buckley KM.** Beamforming: a versatile approach to spatial filtering. *IEEE Assp Mag* 5: 4–24, 1988. doi:10.1109/53.665.
44. **Hillebrand A**, **Barnes GR.** Beamformer analysis of MEG data. *Int Rev Neurobiol* 68: 149–171, 2005. doi:10.1016/S0074-7742(05)68006-3.
45. **Brookes MJ**, **Stevenson CM**, **Barnes GR**, **Hillebrand A**, **Simpson MI**, **Francis ST**, **Morris PG.** Beamformer reconstruction of correlated sources using a modified source model. *NeuroImage* 34: 1454–1465, 2007. doi:10.1016/j.neuroimage.2006.11.012.
46. **Van Veen BD**, **Van Drongelen W**, **Yuchtman M**, **Suzuki A.** Localization of brain electrical activity via linearly constrained minimum variance spatial filtering. *IEEE Trans Biomed Eng* 44: 867–880, 1997. doi:10.1109/10.623056.
47. **Robinson S**, **Vrba J.** Functional neuroimaging by synthetic aperture magnetometry (SAM). In: *Recent Advances in Biomagnetism*. Sendai: Tohoku University Press, 1999, p. 302–305.
48. **Sekihara K**, **Nagarajan SS**, **Poeppel D**, **Marantz A**, **Miyashita Y.** Reconstructing spatio-temporal activities of neural sources using an MEG vector beamformer technique. *IEEE Trans Biomed Eng* 48: 760–771, 2001. doi:10.1109/10.930901.
49. **Huang M-X**, **Shih J**, **Lee R**, **Harrington D**, **Thoma R**, **Weisend M**, **Hanlon F**, **Paulson K**, **Li T**, **Martin K.** Commonalities and differences among vectorized beamformers in electromagnetic source imaging. *Brain Topogr* 16: 139–158, 2004. doi:10.1023/B:BRAT.0000019183.92439.51.
50. **Mosher JC**, **Leahy RM.** Recursive MUSIC: a framework for EEG and MEG source localization. *IEEE Trans Biomed Eng* 45: 1342–1354, 1998. doi:10.1109/10.725331.
51. **Sekihara K**, **Nagarajan S**, **Poeppel D**, **Miyashita Y.** Time-frequency MEG-MUSIC algorithm. *IEEE Trans Med Imaging* 18: 92–97, 1999. doi:10.1109/42.750262.
52. **Schmidt R.** Multiple emitter location and signal parameter estimation. *IEEE Trans Antennas Propagat* 34: 276–280, 1986. doi:10.1109/TAP.1986.1143830.
53. **Taniguchi M**, **Kato A**, **Fujita N**, **Hirata M**, **Tanaka H**, **Kihara T**, **Ninomiya H**, **Hirabuki N**, **Nakamura H**, **Robinson SE**, **Cheyne D**, **Yoshimine T.** Movement-related desynchronization of the cerebral cortex studied with spatially filtered magnetoencephalography. *NeuroImage* 12: 298–306, 2000. doi:10.1006/nimg.2000.0611.
54. **Ishii R**, **Shinosaki K**, **Ukai S**, **Inouye T**, **Ishihara T**, **Yoshimine T**, **Hirabuki N**, **Asada H**, **Kihara T**, **Robinson SE.** Medial prefrontal cortex generates frontal midline theta rhythm. *Neuroreport* 10: 675–679, 1999.
55. **Vrba J**, **Robinson S.** Linearly constrained minimum variance beamformers, synthetic aperture magnetometry, and MUSIC in MEG applications. *Asilomar Conference on Signals, Systems and Computers*. Pacific Grove, CA, October 29–November 1, 2000. doi:10.1109/ACSSC.2000.910969.
56. **Vrba J**, **Robinson S.** Signal processing in magnetoencephalography. *Methods* 25: 249–271, 2001. doi:10.1006/meth.2001.1238.
57. **Cheyne D**, **Bakhtazad L**, **Gaetz W.** Spatiotemporal mapping of cortical activity accompanying voluntary movements using an event-related beamforming approach. *Hum Brain Mapp* 27: 213–229, 2006. doi:10.1002/hbm.20178.
58. **Robinson S.** Localization of event-related activity by SAM(erf). *Neurol Clin Neurophysiol* 2004: 109–109, 2004.
59. **Gross J**, **Kujala J**, **Hämäläinen M**, **Timmermann L**, **Schnitzler A**, **Salmelin R.** Dynamic imaging of coherent sources: studying neural interactions in the human brain. *Proc Natl Acad Sci USA* 98: 694–699, 2001. doi:10.1073/pnas.98.2.694.
60. **Moiseev A**, **Gaspar JM**, **Schneider JA**, **Herdman AT.** Application of multi-source minimum variance beamformers for reconstruction of correlated neural activity. *NeuroImage* 58: 481–496, 2011. doi:10.1016/j.neuroimage.2011.05.081.
61. **Hillebrand A**, **Barnes GR**, **Bosboom JL**, **Berendse HW**, **Stam CJ.** Frequency-dependent functional connectivity within resting-state networks: an atlas-based MEG beamformer solution. *NeuroImage* 59: 3909–3921, 2012. doi:10.1016/j.neuroimage.2011.11.005.
62. **Friston KJ.** Functional and effective connectivity in neuroimaging: a synthesis. *Hum Brain Mapp* 2: 56–78, 1994. doi:10.1002/hbm.460020107.
63. **Friston K**, **Frith C**, **Liddle P**, **Frackowiak R.** Functional connectivity: the principal-component analysis of large (PET) data sets. *J Cereb Blood Flow Metab* 13: 5–14, 1993. doi:10.1038/jcbfm.1993.4.
64. **Aertsen A**, **Preissl H.** Dynamics of activity and connectivity in physiological neuronal networks. In: *Nonlinear Dynamics and Neuronal Networks*, edited by Schuster H. New York: HG VCH Publishers, 1991, p. 281–302.
65. **Aertsen A**, **Gerstein G**, **Habib M**, **Palm G.** Dynamics of neuronal firing correlation: modulation of effective connectivity. *J Neurophysiol* 61: 900–917, 1989. doi:10.1152/jn.1989.61.5.900.
66. **Aertsen AM**, **Gerstein GL.** Evaluation of neuronal connectivity: sensitivity of cross-correlation. *Brain Res* 340: 341–354, 1985. doi:10.1016/0006-8993(85)90931-X.
67. **Gerstein GL**, **Perkel DH.** Mutual temporal relationships among neuronal spike trains: Statistical techniques for display and analysis. *Biophys J* 12: 453–473, 1972. doi:10.1016/S0006-3495(72)86097-1.
68. **Palm G**, **Aertsen A**, **Gerstein G.** On the significance of correlations among neuronal spike trains. *Biol Cybern* 59: 1–11, 1988. doi:10.1007/BF00336885.
69. **Perkel DH**, **Gerstein GL**, **Moore GP.** Neuronal spike trains and stochastic point processes: II. Simultaneous spike trains. *Biophys J* 7: 419–440, 1967. doi:10.1016/S0006-3495(67)86597-4.
70. **Adey WR**, **Walter DO**, **Hendrix C.** Computer techniques in correlation and spectral analyses of cerebral slow waves during discriminative behavior. *Exp Neurol* 3: 501–524, 1961. doi:10.1016/S0014-4886(61)80002-2.
71. **Gevins AS**, **Doyle JC**, **Cutillo BA**, **Schaffer RE**, **Tannehill RS**, **Bressler SL.** Neurocognitive pattern analysis of a visuospatial task: Rapidly-shifting foci of evoked correlations between electrodes. *Psychophysiology* 22: 32–43, 1985. doi:10.1111/j.1469-8986.1985.tb01557.x.
72. **Livanov MN.** *Spatial Organization of Cerebral Processes*. New York: John Wiley & Sons, 1977, p. 181.
73. **Clark CM**, **Kessler R**, **Buchsbaum MS**, **Margolin RA**, **Holcomb HH.** Correlational methods for determining regional coupling of cerebral glucose metabolism: a pilot study. *Biol Psychiatry* 19: 663–678, 1984.
74. **Horwitz B**, **Duara R**, **Rapoport SI.** Intercorrelations of glucose metabolic rates between brain regions: application to healthy males in a state of reduced sensory input. *J Cereb Blood Flow Metab* 4: 484–499, 1984. doi:10.1038/jcbfm.1984.73.
75. **Metter EJ**, **Riege WH**, **Kuhl DE**, **Phelps ME.** Cerebral metabolic relationships for selected brain regions in healthy adults. *J Cereb Blood Flow Metab* 4: 500–506, 1984. doi:10.1038/jcbfm.1984.74.
76. **Biswal BB**, **Zerrin Yetkin F**, **Haughton VM**, **Hyde JS.** Functional connectivity in the motor cortex of resting human brain using echo-planar MRI. *Magn Reson Med* 34: 537–541, 1995. doi:10.1002/mrm.1910340409.
77. **Cordes D**, **Haughton VM**, **Arfanakis K**, **Carew JD**, **Turski PA**, **Moritz CH**, **Quigley MA**, **Meyerand ME.** Frequencies contributing to functional connectivity in the cerebral cortex in "resting-state" data. *Am J Neuroradiol* 22: 1326–1333, 2001.
78. **Raichle ME**, **MacLeod AM**, **Snyder AZ**, **Powers WJ**, **Gusnard DA**, **Shulman GL.** A default mode of brain function. *Proc Natl Acad Sci USA* 98: 676–682, 2001. doi:10.1073/pnas.98.2.676.
79. **Greicius MD**, **Krasnow B**, **Reiss AL**, **Menon V.** Functional connectivity in the resting brain: a network analysis of the default mode hypothesis. *Proc Natl Acad Sci USA* 100: 253–258, 2003. doi:10.1073/pnas.0135058100.
80. **Damoiseaux JS**, **Rombouts S**, **Barkhof F**, **Scheltens P**, **Stam CJ**, **Smith SM**, **Beckmann CF.** Consistent resting-state networks across healthy subjects. *Proc Natl Acad Sci USA* 103: 13848–13853, 2006. doi:10.1073/pnas.0601417103.
81. **Fox MD**, **Snyder AZ**, **Vincent JL**, **Corbetta M**, **Van Essen DC**, **Raichle ME.** The human brain is intrinsically organized into dynamic, anticorrelated functional networks. *Proc Natl Acad Sci USA* 102: 9673–9678, 2005. doi:10.1073/pnas.0504136102.

82. **De Luca M**, **Beckmann CF**, **De Stefano N**, **Matthews PM**, **Smith SM.** fMRI resting state networks define distinct modes of long-distance interactions in the human brain. *NeuroImage* 29: 1359–1367, 2006. doi:10.1016/j.neuroimage.2005.08.035.
83. **Cherkassky VL**, **Kana RK**, **Keller TA**, **Just MA.** Functional connectivity in a baseline resting-state network in autism. *Neuroreport* 17: 1687–1690, 2006. doi:10.1097/01.wnr.0000239956.45448.4c.
84. **Fox MD**, **Greicius M.** Clinical applications of resting state functional connectivity. *Front Syst Neurosci* 4: 19, 2010. doi:10.3389/fnsys.2010.00019.
85. **Greicius MD**, **Supekar K**, **Menon V**, **Dougherty RF.** Resting-state functional connectivity reflects structural connectivity in the default mode network. *Cereb Cortex* 19: 72–78, 2009. doi:10.1093/cercor/bhn059.
86. **Honey CJ**, **Sporns O**, **Cammoun L**, **Gigandet X**, **Thiran JP**, **Meuli R**, **Hagmann P.** Predicting human resting-state functional connectivity from structural connectivity. *Proc Natl Acad Sci USA* 106: 2035–2040, 2009. doi:10.1073/pnas.0811168106.
87. **Bendat JS**, **Piersol AG.** *Random Data: Analysis and Measurement Procedures* (4th ed.). New York: John Wiley & Sons, 2010.
88. **Palva JM**, **Palva S**, **Kaila K.** Phase synchrony among neuronal oscillations in the human cortex. *J Neurosci* 25: 3962–3972, 2005. doi:10.1523/JNEUROSCI.4250-04.2005.
89. **Bruns A**, **Eckhorn R**, **Jokeit H**, **Ebner A.** Amplitude envelope correlation detects coupling among incoherent brain signals. *Neuroreport* 11: 1509–1514, 2000.
90. **Jirsa V**, **Müller V.** Cross-frequency coupling in real and virtual brain networks. *Front Comput Neurosci* 7: 78, 2013. doi:10.3389/fncom.2013.00078.
91. **Srinivasan R**, **Winter WR**, **Ding J**, **Nunez PL.** EEG and MEG coherence: measures of functional connectivity at distinct spatial scales of neocortical dynamics. *J Neurosci Methods* 166: 41–52, 2007. doi:10.1016/j.jneumeth.2007.06.026.
92. **Nunez PL**, **Silberstein RB**, **Shi Z**, **Carpenter MR**, **Srinivasan R**, **Tucker DM**, **Doran SM**, **Cadusch PJ**, **Wijesinghe RS.** EEG coherency II: experimental comparisons of multiple measures. *Clin Neurophysiol* 110: 469–486, 1999. doi:10.1016/S1388-2457(98)00043-1.
93. **Nunez PL**, **Srinivasan R**, **Westdorp AF**, **Wijesinghe RS**, **Tucker DM**, **Silberstein RB**, **Cadusch PJ.** EEG coherency: I: statistics, reference electrode, volume conduction, Laplacians, cortical imaging, and interpretation at multiple scales. *Electroencephalogr Clin Neurophysiol* 103: 499–515, 1997. doi:10.1016/S0013-4694(97)00066-7.
94. **Stam CJ**, **Van Dijk B.** Synchronization likelihood: an unbiased measure of generalized synchronization in multivariate data sets. *Physica D* 163: 236–251, 2002. doi:10.1016/S0167-2789(01)00386-4.
95. **Lachaux JP**, **Rodriguez E**, **Martinerie J**, **Varela FJ.** Measuring phase synchrony in brain signals. *Hum Brain Mapp* 8: 194–208, 1999. doi:10.1002/(SICI)1097-0193(1999)8:4<194::AID-HBM4>3.0.CO;2-C.
96. **Moazami-Goudarzi M**, **Sarnthein J**, **Michels L**, **Moukhtieva R**, **Jeanmonod D.** Enhanced frontal low and high frequency power and synchronization in the resting EEG of parkinsonian patients. *NeuroImage* 41: 985–997, 2008. doi:10.1016/j.neuroimage.2008.03.032.
97. **Roux F**, **Wibral M**, **Singer W**, **Aru J**, **Uhlhaas PJ.** The phase of thalamic alpha activity modulates cortical gamma-band activity: evidence from resting-state MEG recordings. *J Neurosci* 33: 17827–17835, 2013. doi:10.1523/JNEUROSCI.5778-12.2013.
98. **Sadaghiani S**, **Scheeringa R**, **Lehongre K**, **Morillon B**, **Giraud A-L**, **D'Esposito M**, **Kleinschmidt A.** Alpha-band phase synchrony is related to activity in the fronto-parietal adaptive control network. *J Neurosci* 32: 14305–14310, 2012. doi:10.1523/JNEUROSCI.1358-12.2012.
99. **Schlee W**, **Hartmann T**, **Langguth B**, **Weisz N.** Abnormal resting-state cortical coupling in chronic tinnitus. *BMC Neurosci* 10: 11, 2009. doi:10.1186/1471-2202-10-11.
100. **Schmidt BT**, **Ghuman AS**, **Huppert TJ.** Whole brain functional connectivity using phase locking measures of resting state magnetoencephalography. *Front Neurosci* 8: 141, 2014. doi:10.3389/fnins.2014.00141.
101. **Altenburg J**, **Vermeulen RJ**, **Strijers RL**, **Fetter WP**, **Stam CJ.** Seizure detection in the neonatal EEG with synchronization likelihood. *Clin Neurophysiol* 114: 50–55, 2003. doi:10.1016/S1388-2457(02)00322-X.
102. **Pijnenburg YAL**, **V D Made Y**, **van Cappellen van Walsum AM**, **Knol DL**, **Scheltens P**, **Stam CJ.** EEG synchronization likelihood in mild cognitive impairment and Alzheimer's disease during a working memory task. *Clin Neurophysiol* 115: 1332–1339, 2004. doi:10.1016/j.clinph.2003.12.029.
103. **Stam CJ**, **van Walsum AMvC**, **Pijnenburg YA**, **Berendse HW**, **de Munck JC**, **Scheltens P**, **van Dijk BW.** Generalized synchronization of MEG recordings in Alzheimer's disease: evidence for involvement of the gamma band. *J Clin Neurophysiol* 19: 562–574, 2002. doi:10.1097/00004691-200212000-00010.
104. **Stam CJ**, **Nolte G**, **Daffertshofer A.** Phase lag index: assessment of functional connectivity from multi channel EEG and MEG with diminished bias from common sources. *Hum Brain Mapp* 28: 1178–1193, 2007. doi:10.1002/hbm.20346.
105. **Vinck M**, **Oostenveld R**, **Van Wingerden M**, **Battaglia F**, **Pennartz CM.** An improved index of phase-synchronization for electrophysiological data in the presence of volume-conduction, noise and sample-size bias. *NeuroImage* 55: 1548–1565, 2011. doi:10.1016/j.neuroimage.2011.01.055.
106. **Stam CJ**, **van Straaten EC.** Go with the flow: use of a directed phase lag index (dPLI) to characterize patterns of phase relations in a large-scale model of brain dynamics. *NeuroImage* 62: 1415–1428, 2012. doi:10.1016/j.neuroimage.2012.05.050.
107. **Nolte G**, **Bai O**, **Wheaton L**, **Mari Z**, **Vorbach S**, **Hallett M.** Identifying true brain interaction from EEG data using the imaginary part of coherency. *Clin Neurophysiol* 115: 2292–2307, 2004. doi:10.1016/j.clinph.2004.04.029.
108. **Dunkley B**, **Doesburg S**, **Sedge P**, **Grodecki R**, **Shek P**, **Pang E**, **Taylor M.** Resting-state hippocampal connectivity correlates with symptom severity in post-traumatic stress disorder. *NeuroImage Clin* 5: 377–384, 2014. doi:10.1016/j.nicl.2014.07.017.
109. **Kasakawa S**, **Yamanishi T**, **Takahashi T**, **Ueno K**, **Kikuchi M**, **Nishimura H.** Approaches of phase lag index to EEG signals in Alzheimer's disease from complex network analysis. In: *Innovation in Medicine and Healthcare 2015*. Cham, Switzerland: Springer, 2016, p. 459–468.
110. **Polanía R**, **Nitsche MA**, **Korman C**, **Batsikadze G**, **Paulus W.** The importance of timing in segregated theta phase-coupling for cognitive performance. *Curr Biol* 22: 1314–1318, 2012. doi:10.1016/j.cub.2012.05.021.
111. **Tewarie P**, **Balk LJ**, **Hillebrand A**, **Steenwijk MD**, **Uitdehaag BMJ**, **Stam CJ**, **Petzold A.** Structure-function relationships in the visual system in multiple sclerosis: an MEG and OCT study. *Ann Clin Transl Neurol* 4: 614–621, 2017. doi:10.1002/acn3.415.
112. **Tewarie P**, **Schoonheim MM**, **Stam CJ**, **van der Meer ML**, **van Dijk BW**, **Barkhof F**, **Polman CH**, **Hillebrand A.** Cognitive and clinical dysfunction, altered MEG resting-state networks and thalamic atrophy in multiple sclerosis. *PLoS One* 8: e69318, 2013. doi:10.1371/journal.pone.0069318.
113. **van Dellen E**, **Douw L**, **Hillebrand A**, **Ris-Hilgersom IHM**, **Schoonheim MM**, **Baayen JC**, **De Witt Hamer PC**, **Velis DN**, **Klein M**, **Heimans JJ**, **Stam CJ**, **Reijneveld JC.** MEG network differences between low-and high-grade glioma related to epilepsy and cognition. *PLoS One* 7: e50122, 2012. doi:10.1371/journal.pone.0050122.
114. **Brookes MJ**, **Woolrich M**, **Luckhoo H**, **Price D**, **Hale JR**, **Stephenson MC**, **Barnes GR**, **Smith SM**, **Morris PG.** Investigating the electrophysiological basis of resting state networks using magnetoencephalography. *Proc Natl Acad Sci USA* 108: 16783–16788, 2011. doi:10.1073/pnas.1112685108.
115. **Liu Z**, **Fukunaga M**, **de Zwart JA**, **Duyn JH.** Large-scale spontaneous fluctuations and correlations in brain electrical activity observed with magnetoencephalography. *NeuroImage* 51: 102–111, 2010. doi:10.1016/j.neuroimage.2010.01.092.
116. **Brookes MJ**, **Woolrich MW**, **Barnes GR.** Measuring functional connectivity in MEG: a multivariate approach insensitive to linear source leakage. *NeuroImage* 63: 910–920, 2012. doi:10.1016/j.neuroimage.2012.03.048.
117. **Colclough GL**, **Brookes MJ**, **Smith SM**, **Woolrich MW.** A symmetric multivariate leakage correction for MEG connectomes. *NeuroImage* 117: 439–448, 2015. doi:10.1016/j.neuroimage.2015.03.071.
118. **Hipp JF**, **Hawellek DJ**, **Corbetta M**, **Siegel M**, **Engel AK.** Large-scale cortical correlation structure of spontaneous oscillatory activity. *Nat Neurosci* 15: 884–890, 2012. doi:10.1038/nn.3101.

119. **Brookes MJ**, **Hale JR**, **Zumer JM**, **Stevenson CM**, **Francis ST**, **Barnes GR**, **Owen JP**, **Morris PG**, **Nagarajan SS.** Measuring functional connectivity using MEG: methodology and comparison with fcMRI. *NeuroImage* 56: 1082–1104, 2011. doi:10.1016/j.neuroimage.2011.02.054.
120. **Brookes MJ**, **Tewarie PK**, **Hunt BAE**, **Robson SE**, **Gascoyne LE**, **Liddle EB**, **Liddle PF**, **Morris PG.** A multi-layer network approach to MEG connectivity analysis. *NeuroImage* 132: 425–438, 2016. doi:10.1016/j.neuroimage.2016.02.045.
121. **Canolty RT**, **Knight RT.** The functional role of cross-frequency coupling. *Trends Cogn Sci* 14: 506–515, 2010. doi:10.1016/j.tics.2010.09.001.
122. **Jensen O**, **Colgin LL.** Cross-frequency coupling between neuronal oscillations. *Trends Cogn Sci* 11: 267–269, 2007. doi:10.1016/j.tics.2007.05.003.
123. **Palva S**, **Palva JM.** Roles of brain criticality and multiscale oscillations in temporal predictions for sensorimotor processing. *Trends Neurosci* 41: 729–743, 2018. doi:10.1016/j.tins.2018.08.008.
124. **Axmacher N**, **Henseler MM**, **Jensen O**, **Weinreich I**, **Elger CE**, **Fell J.** Cross-frequency coupling supports multi-item working memory in the human hippocampus. *Proc Natl Acad Sci USA* 107: 3228–3233, 2010. doi:10.1073/pnas.0911531107.
125. **Siegel M**, **Warden MR**, **Miller EK.** Phase-dependent neuronal coding of objects in short-term memory. *Proc Natl Acad Sci USA* 106: 21341–21346, 2009. doi:10.1073/pnas.0908193106.
126. **Tort AB**, **Komorowski RW**, **Manns JR**, **Kopell NJ**, **Eichenbaum H.** Theta–gamma coupling increases during the learning of item–context associations. *Proc Natl Acad Sci USA* 106: 20942–20947, 2009. doi:10.1073/pnas.0911331106.
127. **Voytek B**, **Canolty RT**, **Shestyuk A**, **Crone N**, **Parvizi J**, **Knight RT.** Shifts in gamma phase–amplitude coupling frequency from theta to alpha over posterior cortex during visual tasks. *Front Hum Neurosci* 4: 191, 2010. doi:10.3389/fnhum.2010.00191.
128. **Canolty RT**, **Edwards E**, **Dalal SS**, **Soltani M**, **Nagarajan SS**, **Kirsch HE**, **Berger MS**, **Barbaro NM**, **Knight RT.** High gamma power is phase-locked to theta oscillations in human neocortex. *Science* 313: 1626–1628, 2006. doi:10.1126/science.1128115.
129. **Bragin A**, **Jandó G**, **Nádasdy Z**, **Hetke J**, **Wise K**, **Buzsáki G.** Gamma (40-100 Hz) oscillation in the hippocampus of the behaving rat. *J Neurosci* 15: 47–60, 1995. doi:10.1523/JNEUROSCI.15-01-00047.1995.
130. **Soltesz I**, **Deschenes M.** Low-and high-frequency membrane potential oscillations during theta activity in CA1 and CA3 pyramidal neurons of the rat hippocampus under ketamine-xylazine anesthesia. *J Neurophysiol* 70: 97–116, 1993. doi:10.1152/jn.1993.70.1.97.
131. **De Hemptinne C**, **Ryapolova-Webb ES**, **Air EL**, **Garcia PA**, **Miller KJ**, **Ojemann JG**, **Ostrem JL**, **Galifianakis NB**, **Starr PA.** Exaggerated phase–amplitude coupling in the primary motor cortex in Parkinson disease. *Proc Natl Acad Sci USA* 110: 4780–4785, 2013. doi:10.1073/pnas.1214546110.
132. **De Hemptinne C**, **Swann NC**, **Ostrem JL**, **Ryapolova-Webb ES**, **San Luciano M**, **Galifianakis NB**, **Starr PA.** Therapeutic deep brain stimulation reduces cortical phase-amplitude coupling in Parkinson's disease. *Nat Neurosci* 18: 779–786, 2015. doi:10.1038/nn.3997.
133. **Florin E**, **Baillet S.** The brain's resting-state activity is shaped by synchronized cross-frequency coupling of neural oscillations. *NeuroImage* 111: 26–35, 2015. doi:10.1016/j.neuroimage.2015.01.054.
134. **Palva S**, **Palva JM.** Discovering oscillatory interaction networks with M/EEG: challenges and breakthroughs. *Trends Cogn Sci* 16: 219–230, 2012. doi:10.1016/j.tics.2012.02.004.
135. **Colclough GL**, **Woolrich MW**, **Tewarie P**, **Brookes MJ**, **Quinn AJ**, **Smith SM.** How reliable are MEG resting-state connectivity metrics? *NeuroImage* 138: 284–293, 2016. doi:10.1016/j.neuroimage.2016.05.070.
136. **Jin S-H**, **Seol J**, **Kim JS**, **Chung CK.** How reliable are the functional connectivity networks of MEG in resting states? *J Neurophysiol* 106: 2888–2895, 2011. doi:10.1152/jn.00335.2011.
137. **Deuker L**, **Bullmore ET**, **Smith M**, **Christensen S**, **Nathan PJ**, **Rockstroh B**, **Bassett DS.** Reproducibility of graph metrics of human brain functional networks. *NeuroImage* 47: 1460–1468, 2009. doi:10.1016/j.neuroimage.2009.05.035.
138. **Dimitriadis SI**, **Routley B**, **Linden DE**, **Singh K.** Reliability of static and dynamic network metrics in the resting-state: a MEG-beamformed connectivity analysis. *Front Neurosci* 12: 506, 2018.
139. **Bruña R**, **Maestú F**, **Pereda E.** Phase locking value revisited: teaching new tricks to an old dog. *J Neural Eng* 15: 056011, 2018. doi:10.1088/1741-2552/aacfe4.
140. **Palva JM**, **Wang SH**, **Palva S**, **Zhigalov A**, **Monto S**, **Brookes MJ**, **Schoffelen J-M**, **Jerbi K.** Ghost interactions in MEG/EEG source space: A note of caution on inter-areal coupling measures. *NeuroImage* 173: 632–643, 2018. doi:10.1016/j.neuroimage.2018.02.032.
141. **Wang SH**, **Lobier M**, **Siebenhühner F**, **Puoliväli T**, **Palva S**, **Palva JM.** Hyperedge bundling: a practical solution to spurious interactions in MEG/EEG source connectivity analyses. *NeuroImage* 173: 610–622, 2018. doi:10.1016/j.neuroimage.2018.01.056.
142. **Ashrafulla S**, **Pantazis D**, **Mosher J**, **Hämäläinen M**, **Liu B**, **Leahy RM.** Viability of sharing MEG data using minimum-norm imaging. Medical Imaging. Advanced PACS-based Imaging Informatics and Therapeutic Applications. Lake Buena Vista, FL, February 16–17, 2011.
143. **Bardouille T**, **Power L**, **Lalancette M**, **Bishop R**, **Beyea S**, **Taylor MJ**, **Dunkley BT.** Variability and bias between magnetoencephalography systems in non-invasive localization of the primary somatosensory cortex. *Clin Neurol Neurosurg* 171: 63–69, 2018. doi:10.1016/j.clineuro.2018.05.018.
144. **Ou W**, **Golland P**, **Hämäläinen M.** Sources of variability in MEG. In: *International Conference on Medical Image Computing and Computer-Assisted Intervention*. New York: Springer, 2007, p. 751–759.
145. **Hari R**, **Baillet S**, **Barnes G**, **Burgess R**, **Forss N**, **Gross J**, **Hamalainen M**, **Jensen O**, **Kakigi R**, **Mauguiere F**, **Nakasato N**, **Puce A**, **Romani GL**, **Schnitzler A**, **Taulu S.** IFCN-endorsed practical guidelines for clinical magnetoencephalography (MEG). *Clin Neurophysiol* 129: 1720–1747, 2018. doi:10.1016/j.clinph.2018.03.042.
146. **Kirsch HE**, **Mantle M**, **Nagarajan SS.** Concordance between routine interictal magnetoencephalography and simultaneous scalp electroencephalography in a sample of patients with epilepsy. *J Clin Neurophysiol* 24: 215, 2007. doi:10.1097/WNP.0b013e3180556095.
147. **Lin YY**, **Shih YH**, **Hsieh JC**, **Yu HY**, **Yiu CH**, **Wong TT**, **Yeh TC**, **Kwan SY**, **Ho LT**, **Yen DJ**, **Wu ZA**, **Chang MS.** Magnetoencephalographic yield of interictal spikes in temporal lobe epilepsy: comparison with scalp EEG recordings. *NeuroImage* 19: 1115–1126, 2003. doi:10.1016/S1053-8119(03)00181-2.
148. **Pataraia E**, **Lindinger G**, **Deecke L**, **Mayer D**, **Baumgartner C.** Combined MEG/EEG analysis of the interictal spike complex in mesial temporal lobe epilepsy. *NeuroImage* 24: 607–614, 2005. doi:10.1016/j.neuroimage.2004.09.031.
149. **Fischer MJ**, **Scheler G**, **Stefan H.** Utilization of magnetoencephalography results to obtain favourable outcomes in epilepsy surgery. *Brain* 128: 153–157, 2005. doi:10.1093/brain/awh333.
150. **Knake S**, **Halgren E**, **Shiraishi H**, **Hara K**, **Hamer HM**, **Grant PE**, **Carr VA**, **Foxe D**, **Camposano S**, **Busa E**, **Witzel T**, **Hämäläinen MS**, **Ahlfors SP**, **Bromfield EB**, **Black PM**, **Bourgeois BF**, **Cole AJ**, **Cosgrove GR**, **Dworetzky BA**, **Madsen JR**, **Larsson PG**, **Schomer DL**, **Thiele EA**, **Dale AM**, **Rosen BR**, **Stufflebeam SM.** The value of multichannel MEG and EEG in the presurgical evaluation of 70 epilepsy patients. *Epilepsy Res* 69: 80–86, 2006. doi:10.1016/j.eplepsyres.2006.01.001.
151. **Knowlton RC.** The role of FDG-PET, ictal SPECT, and MEG in the epilepsy surgery evaluation. *Epilepsy Behav* 8: 91–101, 2006. doi:10.1016/j.yebeh.2005.10.015.
152. **Otsubo H**, **Ochi A**, **Elliott I**, **Chuang SH**, **Rutka JT**, **Jay V**, **Aung M**, **Sobel DF**, **Snead OC III.** MEG predicts epileptic zone in lesional extrahippocampal epilepsy: 12 pediatric surgery cases. *Epilepsia* 42: 1523–1530, 2001. doi:10.1046/j.1528-1157.2001.16701.x.
153. **RamachandranNair R**, **Otsubo H**, **Shroff MM**, **Ochi A**, **Weiss SK**, **Rutka JT**, **Snead III OC.** MEG predicts outcome following surgery for intractable epilepsy in children with normal or nonfocal MRI findings. *Epilepsia* 48: 149–157, 2007. doi:10.1111/j.1528-1167.2006.00901.x.
154. **Hirata M**, **Goto T**, **Barnes G**, **Umekawa Y**, **Yanagisawa T**, **Kato A**, **Oshino S**, **Kishima H**, **Hashimoto N**, **Saitoh Y**, **Tani N**, **Yorifuji S**, **Yoshimine T.** Language dominance and mapping based on neuromagnetic oscillatory changes: comparison with invasive procedures. *J Neurosurg* 112: 528–538, 2010. doi:10.3171/2009.7.JNS09239.
155. **Kim JS**, **Chung CK.** Language lateralization using MEG beta frequency desynchronization during auditory oddball stimulation with

one-syllable words. *NeuroImage* 42: 1499–1507, 2008. doi:10.1016/j.neuroimage.2008.06.001.

156. **Papanicolaou AC**, **Rezaie R**, **Narayana S**, **Choudhri AF**, **Wheless JW**, **Castillo EM**, **Baumgartner JE**, **Boop FA.** Is it time to replace the Wada test and put awake craniotomy to sleep? *Epilepsia* 55: 629–632, 2014. doi:10.1111/epi.12569.
157. **Papanicolaou AC**, **Simos PG**, **Castillo EM**, **Breier JI**, **Sarkari S**, **Pataraia E**, **Billingsley RL**, **Buchanan S**, **Wheless J**, **Maggio V**, **Maggio WW.** Magnetocephalography: a noninvasive alternative to the Wada procedure. *J Neurosurg* 100: 867–876, 2004. doi:10.3171/jns.2004.100.5.0867.
158. **Garcia-Ramos C**, **Song J**, **Hermann B**, **Prabhakaran V.** Low functional robustness in mesial temporal lobe epilepsy. *Epilepsy Res* 123: 20–28, 2016. doi:10.1016/j.eplepsyres.2016.04.001.
159. **Pourmotabbed H**, **Wheless JW**, **Babajani-Feremi A.** Lateralization of epilepsy using intra-hemispheric brain networks based on resting-state MEG data. *Hum Brain Mapp* 41: 2964–2979, 2020. doi:10.1002/hbm.24990.
160. **Van Mierlo P**, **Höller Y**, **Focke NK**, **Vulliemoz S.** Network perspectives on epilepsy using EEG/MEG source connectivity. *Front Neurol* 10: 721, 2019. doi:10.3389/fneur.2019.00721.
161. **Chowdhury RA**, **Pellegrino G**, **Aydin Û**, **Lina JM**, **Dubeau F**, **Kobayashi E**, **Grova C.** Reproducibility of EEG-MEG fusion source analysis of interictal spikes: relevance in presurgical evaluation of epilepsy. *Hum Brain Mapp* 39: 880–901, 2018. doi:10.1002/hbm.23889.
162. **Duez L**, **Tankisi H**, **Hansen PO**, **Sidenius P**, **Sabers A**, **Pinborg LH**, **Fabricius M**, **Rásonyi G**, **Rubboli G**, **Pedersen B**, **Leffers A-M**, **Uldall P**, **Jespersen B**, **Brennum J**, **Henriksen OM**, **Fuglsang-Frederiksen A**, **Beniczky S.** Electromagnetic source imaging in presurgical workup of patients with epilepsy: a prospective study. *Neurology* 92: e576–e586, 2019. doi:10.1212/WNL.0000000000006877.
163. **Foged MT**, **Martens T**, **Pinborg LH**, **Hamrouni N**, **Litman M**, **Rubboli G**, **Leffers A-M**, **Ryvlin P**, **Jespersen B**, **Paulson OB**, **Fabricius M**, **Beniczky S.** Diagnostic added value of electrical source imaging in presurgical evaluation of patients with epilepsy: a prospective study. *Clin Neurophysiol* 131: 324–329, 2020. doi:10.1016/j.clinph.2019.07.031.
164. **Plummer C**, **Vogrin SJ**, **Woods WP**, **Murphy MA**, **Cook MJ**, **Liley DT.** Interictal and ictal source localization for epilepsy surgery using high-density EEG with MEG: a prospective long-term study. *Brain* 142: 932–951, 2019. doi:10.1093/brain/awz015.
165. **Rampp S**, **Stefan H**, **Wu X**, **Kaltenhäuser M**, **Maess B**, **Schmitt FC**, **Wolters CH**, **Hamer H**, **Kasper BS**, **Schwab S**, **Doerfler A**, **Blümcke I**, **Rössler K**, **Buchfelder M.** Magnetoencephalography for epileptic focus localization in a series of 1000 cases. *Brain* 142: 3059–3071, 2019. doi:10.1093/brain/awz231.
166. **Velmurugan J**, **Nagarajan SS**, **Mariyappa N**, **Mundlamuri RC**, **Raghavendra K**, **Bharath RD**, **Saini J**, **Arivazhagan A**, **Rajeswaran J**, **Mahadevan A**, **Malla BR**, **Satishchandra P**, **Sinha S.** Magnetoencephalography imaging of high frequency oscillations strengthens presurgical localization and outcome prediction. *Brain* 142: 3514–3529, 2019. doi:10.1093/brain/awz284.
167. **Engels MM**, **Hillebrand A**, **van der Flier WM**, **Stam CJ**, **Scheltens P**, **van Straaten EC.** Slowing of hippocampal activity correlates with cognitive decline in early onset Alzheimer's disease. An MEG study with virtual electrodes. *Front Hum Neurosci* 10: 238, 2016. doi:10.3389/fnhum.2016.00238.
168. **Kim JA**, **Bosma RL**, **Hemington KS**, **Rogachov A**, **Osborne NR**, **Cheng JC**, **Oh J**, **Dunkley BT**, **Davis KD.** Cross-network coupling of neural oscillations in the dynamic pain connectome reflects chronic neuropathic pain in multiple sclerosis. *NeuroImage Clin* 26: 102230, 2020. doi:10.1016/j.nicl.2020.102230.
169. **Huang J-C**, **Nicholson C**, **Okada YC.** Distortion of magnetic evoked fields and surface potentials by conductivity differences at boundaries in brain tissue. *Biophys J* 57: 1155–1166, 1990. doi:10.1016/S0006-3495(90)82635-7.
170. **Tecchio F**, **Zappasodi F**, **Pasqualetti P**, **Tombini M**, **Caulo M**, **Ercolani M**, **Rossini P.** Long-term effects of stroke on neuronal rest activity in rolandic cortical areas. *J Neurosci Res* 83: 1077–1087, 2006. doi:10.1002/jnr.20796.
171. **Tecchio F**, **Zappasodi F**, **Pasqualetti P**, **Tombini M**, **Salustri C**, **Oliviero A**, **Pizzella V**, **Vernieri F**, **Rossini PM.** Rhythmic brain activity at rest from rolandic areas in acute mono-hemispheric stroke: a magnetoencephalographic study. *NeuroImage* 28: 72–83, 2005. doi:10.1016/j.neuroimage.2005.05.051.
172. **Zappasodi F**, **Tombini M**, **Milazzo D**, **Rossini PM**, **Tecchio F.** Delta dipole density and strength in acute monohemispheric stroke. *Neurosci Lett* 416: 310–314, 2007. doi:10.1016/j.neulet.2007.02.017.
173. **Altamura C**, **Torquati K**, **Zappasodi F**, **Ferretti A**, **Pizzella V**, **Tibuzzi F**, **Vernieri F**, **Pasqualetti P**, **Landi D**, **Del Gratta C**, **Romani G-L**, **Maria Rossini P**, **Tecchio F.** fMRI-vs-MEG evaluation of post-stroke interhemispheric asymmetries in primary sensorimotor hand areas. *Exp Neurol* 204: 631–639, 2007. doi:10.1016/j.expneurol.2006.12.017.
174. **Chu RK**, **Braun AR**, **Meltzer JA.** MEG-based detection and localization of perilesional dysfunction in chronic stroke. *NeuroImage Clin* 8: 157–169, 2015. doi:10.1016/j.nicl.2015.03.019.
175. **Huang M**, **Davis LE**, **Aine C**, **Weisend M**, **Harrington D**, **Christner R**, **Stephen J**, **Edgar JC**, **Herman M**, **Meyer J**, **Paulson K**, **Martin K**, **Lee RR.** MEG response to median nerve stimulation correlates with recovery of sensory and motor function after stroke. *Clin Neurophysiol* 115: 820–833, 2004. doi:10.1016/j.clinph.2003.11.022.
176. **Rossini P**, **Caltagirone C**, **Castriota-Scanderbeg A**, **Cicinelli P**, **Del Gratta C**, **Demartin M**, **Pizzella V**, **Traversa R**, **Romani G.** Hand motor cortical area reorganization in stroke: a study with fMRI, MEG and TCS maps. *Neuroreport* 9: 2141–2146, 1998. doi:10.1097/00001756-199806220-00043.
177. **Rossini PM**, **Tecchio F**, **Pizzella V**, **Lupoi D**, **Cassetta E**, **Pasqualetti P**, **Paqualetti P.** Interhemispheric differences of sensory hand areas after monohemispheric stroke: MEG/MRI integrative study. *NeuroImage* 14: 474–485, 2001 [Erratum in *NeuroImage* 14: 1230, 2001]. doi:10.1006/nimg.2000.0686.
178. **Shih T-y**, **Wu C-y**, **Lin K-C**, **Cheng C-h**, **Hsieh Y-W**, **Chen C-L**, **Lai C-J**, **Chen C-C.** Effects of action observation therapy and mirror therapy after stroke on rehabilitation outcomes and neural mechanisms by MEG: study protocol for a randomized controlled trial. *Trials* 18: 1–8, 2017. doi:10.1186/s13063-017-2205-z.
179. **Tecchio F**, **Zappasodi F**, **Tombini M**, **Caulo M**, **Vernieri F**, **Rossini PM.** Interhemispheric asymmetry of primary hand representation and recovery after stroke: a MEG study. *NeuroImage* 36: 1057–1064, 2007. doi:10.1016/j.neuroimage.2007.02.058.
180. **Tecchio F**, **Zappasodi F**, **Tombini M**, **Oliviero A**, **Pasqualetti P**, **Vernieri F**, **Ercolani M**, **Pizzella V**, **Rossini PM.** Brain plasticity in recovery from stroke: an MEG assessment. *NeuroImage* 32: 1326–1334, 2006. doi:10.1016/j.neuroimage.2006.05.004.
181. **Kielar A**, **Deschamps T**, **Jokel R**, **Meltzer JA.** Functional reorganization of language networks for semantics and syntax in chronic stroke: evidence from MEG. *Hum Brain Mapp* 37: 2869–2893, 2016. doi:10.1002/hbm.23212.
182. **Mohr B**, **MacGregor LJ**, **Difrancesco S**, **Harrington K**, **Pulvermüller F**, **Shtyrov Y.** Hemispheric contributions to language reorganisation: an MEG study of neuroplasticity in chronic post stroke aphasia. *Neuropsychologia* 93: 413–424, 2016. doi:10.1016/j.neuropsychologia.2016.04.006.
183. **Lee RR**, **Huang M.** Magnetoencephalography in the diagnosis of concussion. In: *Concussion*. Basel: Karger Publishers, 2014, p. 94–111.
184. **Antonakakis M**, **Dimitriadis SI**, **Zervakis M**, **Micheloyannis S**, **Rezaie R**, **Babajani-Feremi A**, **Zouridakis G**, **Papanicolaou AC.** Altered cross-frequency coupling in resting-state MEG after mild traumatic brain injury. *Int J Psychophysiol* 102: 1–11, 2016. doi:10.1016/j.ijpsycho.2016.02.002.
185. **Antonakakis M**, **Dimitriadis SI**, **Zervakis M**, **Papanicolaou AC**, **Zouridakis G.** Altered rich-club and frequency-dependent subnetwork organization in mild traumatic brain injury: a MEG resting-state study. *Front Hum Neurosci* 11: 416, 2017.
186. **Antonakakis M**, **Dimitriadis SI**, **Zervakis M**, **Papanicolaou AC**, **Zouridakis G.** Reconfiguration of dominant coupling modes in mild traumatic brain injury mediated by δ-band activity: a resting state MEG study. *Neuroscience* 356: 275–286, 2017. doi:10.1016/j.neuroscience.2017.05.032.
187. **Dunkley BT**, **Urban K**, **Da Costa L**, **Wong SM**, **Pang EW**, **Taylor MJ.** Default mode network oscillatory coupling is increased following concussion. *Front Neurol* 9: 280, 2018. doi:10.3389/fneur.2018.00280.
188. **Huang M-X**, **Huang CW**, **Harrington DL**, **Nichols S**, **Robb-Swan A**, **Angeles-Quinto A**, **Le L**, **Rimmele C**, **Drake A**, **Song T**, **Huang JW**, **Clifford R**, **Ji Z**, **Cheng C-K**, **Lerman I**, **Yurgil KA**, **Lee RR**, **Baker DG.**

Marked increases in resting-state MEG gamma-band activity in combat-related mild traumatic brain injury. *Cereb Cortex* 30: 283–295, 2020. doi:10.1093/cercor/bhz087.

189. **Huang M-X**, **Nichols S**, **Baker DG**, **Robb A**, **Angeles A**, **Yurgil KA**, **Drake A**, **Levy M**, **Song T**, **McLay R.** Single-subject-based whole-brain MEG slow-wave imaging approach for detecting abnormality in patients with mild traumatic brain injury. *NeuroImage Clin* 5: 109–119, 2014. doi:10.1016/j.nicl.2014.06.004.
190. **Huang M-X**, **Nichols S**, **Robb-Swan A**, **Angeles-Quinto A**, **Harrington DL**, **Drake A**, **Huang CW**, **Song T**, **Diwakar M**, **Risbrough VB.** MEG working memory n-back task reveals functional deficits in combat-related mild traumatic brain injury. *Cereb Cortex* 29: 1953–1968, 2019. doi:10.1093/cercor/bhy075.
191. **Huang M-X**, **Risling M**, **Baker DG.** The role of biomarkers and MEG-based imaging markers in the diagnosis of post-traumatic stress disorder and blast-induced mild traumatic brain injury. *Psychoneuroendocrinology* 63: 398–409, 2016. doi:10.1016/j.psyneuen.2015.02.008.
192. **Pang EW**, **Dunkley BT**, **Doesburg SM**, **da Costa L**, **Taylor MJ.** Reduced brain connectivity and mental flexibility in mild traumatic brain injury. *Ann Clin Transl Neurol* 3: 124–131, 2016. doi:10.1002/acn3.280.
193. **Zhou Y**, **Lui YW**, **Zuo XN**, **Milham MP**, **Reaume J**, **Grossman RI**, **Ge Y.** Characterization of thalamo-cortical association using amplitude and connectivity of functional MRI in mild traumatic brain injury. *J Magn Reson Imaging* 39: 1558–1568, 2014. doi:10.1002/jmri.24310.
194. **Zouridakis G**, **Patidar U**, **Pollonini L**, **Situ N**, **Rezaie R**, **Castillo EM**, **Levin HS**, **Papanicolaou AC.** Default brain connectivity network in mild traumatic brain injury—preliminary MEG results. 2011 1st Middle East Conference on Biomedical Engineering. Sharjah, United Arab Emirates, February 21–24. 2011.
195. **Huang M-X**, **Swan AR**, **Quinto AA**, **Matthews S**, **Harrington DL**, **Nichols S**, **Bruder BJ**, **Snook CC**, **Huang CW**, **Baker DG.** A pilot treatment study for mild traumatic brain injury: neuroimaging changes detected by MEG after low-intensity pulse-based transcranial electrical stimulation. *Brain Inj* 31: 1951–1963, 2017. doi:10.1080/02699052.2017.1363409.
196. **Jiang H**, **Popov T**, **Jylänki P**, **Bi K**, **Yao Z**, **Lu Q**, **Jensen O**, **Van Gerven M.** Predictability of depression severity based on posterior alpha oscillations. *Clin Neurophysiol* 127: 2108–2114, 2016. doi:10.1016/j.clinph.2015.12.018.
197. **Lu Q**, **Bi K**, **Liu C**, **Luo G**, **Tang H**, **Yao Z.** Predicting depression based on dynamic regional connectivity: a windowed Granger causality analysis of MEG recordings. *Brain Res* 1535: 52–60, 2013. doi:10.1016/j.brainres.2013.08.033.
198. **Alamian G**, **Hincapié A-S**, **Combrisson E**, **Thiery T**, **Martel V**, **Althukov D**, **Jerbi K.** Alterations of intrinsic brain connectivity patterns in depression and bipolar disorders: a critical assessment of magnetoencephalography-based evidence. *Front Psychiatry* 8: 41, 2017. doi:10.3389/fpsyt.2017.00041.
199. **Bi K**, **Hua L**, **Wei M**, **Qin J**, **Lu Q**, **Yao Z.** Dynamic functional–structural coupling within acute functional state change phases: evidence from a depression recognition study. *J Affect Disord* 191: 145–155, 2016. doi:10.1016/j.jad.2015.11.041.
200. **Kähkönen S**, **Yamashita H**, **Rytsälä H**, **Suominen K**, **Ahveninen J**, **Isometsä E.** Dysfunction in early auditory processing in major depressive disorder revealed by combined MEG and EEG. *J Psychiatry Neurosci* 32: 316, 2007.
201. **Lu Q**, **Li H**, **Luo G**, **Wang Y**, **Tang H**, **Han L**, **Yao Z.** Impaired prefrontal–amygdala effective connectivity is responsible for the dysfunction of emotion process in major depressive disorder: a dynamic causal modeling study on MEG. *Neurosci Lett* 523: 125–130, 2012. doi:10.1016/j.neulet.2012.06.058.
202. **Ye Q**, **Yan D**, **Yao M**, **Lou W**, **Peng W.** Hyperexcitability of cortical oscillations in patients with somatoform pain disorder: a resting-state EEG study. *Neural Plast* 2019: 2687150, 2019. doi:10.1155/2019/2687150.
203. **Moreno-Ortega M**, **Prudic J**, **Rowny S**, **Patel GH**, **Kangarlu A**, **Lee S**, **Grinband J**, **Palomo T**, **Perera T**, **Glasser MF**, **Javitt DC.** Resting state functional connectivity predictors of treatment response to electroconvulsive therapy in depression. *Sci Rep* 9: 5071, 2019. doi:10.1038/s41598-019-41175-4.
204. **Nugent AC**, **Robinson SE**, **Coppola R**, **Zarate CA. Jr**,Preliminary differences in resting state MEG functional connectivity pre-and post-ketamine in major depressive disorder**.** *Psychiatry Res Neuroimaging* 254: 56–66, 2016. doi:10.1016/j.pscychresns.2016.06.006.
205. **Hirano Y**, **Hirano S**, **Maekawa T**, **Obayashi C**, **Oribe N**, **Monji A**, **Kasai K**, **Kanba S**, **Onitsuka T.** Auditory gating deficit to human voices in schizophrenia: a MEG study. *Schizophr Res* 117: 61–67, 2010. doi:10.1016/j.schres.2009.09.003.
206. **Huang M-X**, **Lee RR**, **Gaa KM**, **Song T**, **Harrington DL**, **Loh C**, **Theilmann RJ**, **Edgar JC**, **Miller GA**, **Canive JM**, **Granholm E.** Somatosensory system deficits in schizophrenia revealed by MEG during a median-nerve oddball task. *Brain Topogr* 23: 82–104, 2010. doi:10.1007/s10548-009-0122-5.
207. **Kissler J**, **Müller MM**, **Fehr T**, **Rockstroh B**, **Elbert T.** MEG gamma band activity in schizophrenia patients and healthy subjects in a mental arithmetic task and at rest. *Clin Neurophysiol* 111: 2079–2087, 2000. doi:10.1016/S1388-2457(00)00425-9.
208. **Koh Y**, **Shin KS**, **Kim JS**, **Choi J-S**, **Kang D-H**, **Jang JH**, **Cho K-H**, **O'Donnell BF**, **Chung CK**, **Kwon JS.** An MEG study of alpha modulation in patients with schizophrenia and in subjects at high risk of developing psychosis. *Schizophr Res* 126: 36–42, 2011. doi:10.1016/j.schres.2010.10.001.
209. **Sanfratello L**, **Houck JM**, **Calhoun VD.** Dynamic functional network connectivity in schizophrenia with magnetoencephalography and functional magnetic resonance limaging: do different timescales ell a different story? *Brain Connect* 9: 251–262, 2019. doi:10.1089/brain.2018.0608.
210. **Sanfratello L**, **Houck JM**, **Calhoun VD.** Relationship between MEG global dynamic functional network connectivity measures and symptoms in schizophrenia. *Schizophr Res* 209: 129–134, 2019. doi:10.1016/j.schres.2019.05.007.
211. **Alamian G**, **Hincapié A-S**, **Pascarella A**, **Thiery T**, **Combrisson E**, **Saive A-L**, **Martel V**, **Althukov D**, **Haesebaert F**, **Jerbi K.** Measuring alterations in oscillatory brain networks in schizophrenia with resting-state MEG: State-of-the-art and methodological challenges. *Clin Neurophysiol* 128: 1719–1736, 2017. doi:10.1016/j.clinph.2017.06.246.
212. **Cetin MS**, **Houck JM**, **Rashid B**, **Agacoglu O**, **Stephen JM**, **Sui J**, **Canive J**, **Mayer A**, **Aine C**, **Bustillo JR**, **Calhoun VD.** Multimodal classification of schizophrenia patients with MEG and fMRI data using static and dynamic connectivity measures. *Front Neurosci* 10: 466, 2016. doi:10.3389/fnins.2016.00466.
213. **Gage NM**, **Siegel B**, **Roberts TP.** Cortical auditory system maturational abnormalities in children with autism disorder: an MEG investigation. *Brain Res Dev Brain Res* 144: 201–209, 2003. doi:10.1016/S0165-3806(03)00172-X.
214. **Gage NM**, **Siegel B**, **Callen M**, **Roberts TP.** Cortical sound processing in children with autism disorder: an MEG investigation. *Neuroreport* 14: 2047–2051, 2003. doi:10.1097/00001756-200311140-00008.
215. **Marco EJ**, **Khatibi K**, **Hill SS**, **Siegel B**, **Arroyo MS**, **Dowling AF**, **Neuhaus JM**, **Sherr EH**, **Hinkley LN**, **Nagarajan SS.** Children with autism show reduced somatosensory response: an MEG study. *Autism Res* 5: 340–351, 2012. doi:10.1002/aur.1247.
216. **Roberts TPL**, **Khan SY**, **Rey M**, **Monroe JF**, **Cannon K**, **Blaskey L**, **Woldoff S**, **Qasmieh S**, **Gandal M**, **Schmidt GL**, **Zarnow DM**, **Levy SE**, **Edgar JC.** MEG detection of delayed auditory evoked responses in autism spectrum disorders: towards an imaging biomarker for autism. *Autism Res* 3: 8–18, 2010. doi:10.1002/aur.111.
217. **Tsiaras V**, **Simos PG**, **Rezaie R**, **Sheth BR**, **Garyfallidis E**, **Castillo EM**, **Papanicolaou AC.** Extracting biomarkers of autism from MEG resting-state functional connectivity networks. *Comput Biol Med* 41: 1166–1177, 2011. doi:10.1016/j.compbiomed.2011.04.004.
218. **Wilson TW**, **Rojas DC**, **Reite ML**, **Teale PD**, **Rogers SJ.** Children and adolescents with autism exhibit reduced MEG steady-state gamma responses. *Biol Psychiatry* 62: 192–197, 2007. doi:10.1016/j.biopsych.2006.07.002.
219. **O'Reilly C**, **Lewis JD**, **Elsabbagh M.** Is functional brain connectivity atypical in autism? A systematic review of EEG and MEG studies. *PLoS One* 12: e0175870, 2017. doi:10.1371/journal.pone.0175870.
220. **Safar K**, **Taylor MJ**, **Matsuzaki J**, **Roberts TP.** Applications of magnetoencephalography to autism spectrum disorder. In: *Fifty Years of Magnetoencephalography: Beginnings, Technical Advances, and Applications*, edited by Papanicolaou AC, Roberts TL, Wheless JW. London: Oxford University Press, 2020, p**.** 317.
221. **Gómez C**, **Hornero R.** Entropy and complexity analyses in Alzheimer's disease: an MEG study. *Open Biomed Eng J* 4: 223–235, 2010. doi:10.2174/1874120701004010223.

222. **Gómez C**, **Mediavilla Á**, **Hornero R**, **Abásolo D**, **Fernández A.** Use of the Higuchi's fractal dimension for the analysis of MEG recordings from Alzheimer's disease patients. *Med Eng Phys* 31: 306–313, 2009.
223. **Hornero R**, **Escudero J**, **Fernández A**, **Poza J**, **Gómez C.** Spectral and nonlinear analyses of MEG background activity in patients with Alzheimer's disease. *IEEE Trans Biomed Eng* 55: 1658–1665, 2008. doi:10.1109/tbme.2008.919872.
224. **Poza J**, **Hornero R**, **Abásolo D**, **Fernández A**, **García M.** Extraction of spectral based measures from MEG background oscillations in Alzheimer's disease. *Med Eng Phys* 29: 1073–1083, 2007. doi:10.1016/j.medengphy.2006.11.006.
225. **van Walsum A-MvC**, **Pijnenburg Y**, **Berendse H**, **van Dijk B**, **Knol D**, **Scheltens P**, **Stam C.** A neural complexity measure applied to MEG data in Alzheimer's disease. *Clin Neurophysiol* 114: 1034–1040, 2003. doi:10.1016/S1388-2457(03)00072-5.
226. **Yu M**, **Engels MM**, **Hillebrand A**, **Van Straaten EC**, **Gouw AA**, **Teunissen C**, **Van Der Flier WM**, **Scheltens P**, **Stam CJ.** Selective impairment of hippocampus and posterior hub areas in Alzheimer's disease: an MEG-based multiplex network study. *Brain* 140: 1466–1485, 2017. doi:10.1093/brain/awx050.
227. **López-Sanz D**, **Bruña R**, **Garcés P**, **Camara C**, **Serrano N**, **Rodríguez-Rojo IC**, **Delgado ML**, **Montenegro M**, **López-Higes R**, **Yus M**, **Maestú F.** Alpha band disruption in the AD-continuum starts in the subjective cognitive decline stage: a MEG study. *Sci Rep* 6: 37685, 2016. doi:10.1038/srep37685.
228. **Shumbayawonda E**, **López-Sanz D**, **Bruña R**, **Serrano N**, **Fernández A**, **Maestú F**, **Abasolo D.** Complexity changes in preclinical Alzheimer's disease: an MEG study of subjective cognitive decline and mild cognitive impairment. *Clin Neurophysiol* 131: 437–445, 2020. doi:10.1016/j.clinph.2019.11.023.
229. **Nakamura A**, **Cuesta P**, **Fernández A**, **Arahata Y**, **Iwata K**, **Kuratsubo I**, **Bundo M**, **Hattori H**, **Sakurai T**, **Fukuda K**, **Washimi Y**, **Endo H**, **Takeda A**, **Diers K**, **Bajo R**, **Maestú F**, **Ito K**, **Kat T.** Electromagnetic signatures of the preclinical and prodromal stages of Alzheimer's disease. *Brain* 141: 1470–1485, 2018. doi:10.1093/brain/awy044.
230. **Lopez-Martin M**, **Nevado A**, **Carro B.** Detection of early stages of Alzheimer's disease based on MEG activity with a randomized convolutional neural network. *Artif Intell Med* 107: 101924, 2020. doi:10.1016/j.artmed.2020.101924.
231. **Maestú F**, **Peña J-M**, **Garcés P**, **González S**, **Bajo R**, **Bagic A**, **Cuesta P**, **Funke M**, **Mäkelä JP**, **Menasalvas E**, **Nakamura A**, **Parkkonen L**, **López ME**, **del Pozo F**, **Sudre G**, **Zamrini E**, **Pekkonen E**, **Henson RN**, **Becker , JT**; **Magnetoencephalography International Consortium of Alzheimer's Disease.** A multicenter study of the early detection of synaptic dysfunction in mild cognitive impairment using magnetoencephalography-derived functional connectivity. *NeuroImage Clin* 9: 103–109, 2015. doi:10.1016/j.nicl.2015.07.011.
232. **Juottonen K**, **Gockel M**, **Silén T**, **Hurri H**, **Hari R**, **Forss N.** Altered central sensorimotor processing in patients with complex regional pain syndrome. *Pain* 98: 315–323, 2002. doi:10.1016/S0304-3959(02)00119-7.
233. **Maihöfner C**, **Handwerker HO**, **Neundörfer B**, **Birklein F.** Patterns of cortical reorganization in complex regional pain syndrome. *Neurology* 61: 1707–1715, 2003. doi:10.1212/01.wnl.0000098939.02752.8e.
234. **Walton K**, **Dubois M**, **Llinas R.** Abnormal thalamocortical activity in patients with Complex Regional Pain Syndrome (CRPS) type I. *Pain* 150: 41–51, 2010. doi:10.1016/j.pain.2010.02.023.
235. **Choe MK**, **Lim M**, **Kim JS**, **Lee DS**, **Chung CK.** Disrupted resting state network of fibromyalgia in theta frequency. *Sci Rep* 8: 2064, 2018. doi:10.1038/s41598-017-18999-z.
236. **Hsiao F-J**, **Wang S-J**, **Lin Y-Y**, **Fuh J-L**, **Ko Y-C**, **Wang P-N**, **Chen W-T.** Altered insula–default mode network connectivity in fibromyalgia: a resting-state magnetoencephalographic study. *J Headache Pain* 18: 89, 2017. doi:10.1186/s10194-017-0799-x.
237. **Lim M**, **Kim JS**, **Kim DJ**, **Chung CK.** Increased low- and high-frequency oscillatory activity in the prefrontal cortex of fibromyalgia patients. *Front Hum Neurosci* 10: 111, 2016. doi:10.3389/fnhum.2016.00111.
238. **Maestu C**, **Cortes A**, **Vazquez JM**, **del Rio D**, **Gomez-Arguelles JM**, **del Pozo F**, **Nevado A.** Increased brain responses during subjectively-matched mechanical pain stimulation in fibromyalgia patients as evidenced by MEG. *Clin Neurophysiol* 124: 752–760, 2013. doi:10.1016/j.clinph.2012.09.015.
239. **Guo X**, **Xiang J**, **Wang Y**, **O'Brien H**, **Kabbouche M**, **Horn P**, **Powers SW**, **Hershey AD.** Aberrant neuromagnetic activation in the motor cortex in children with acute migraine: a magnetoencephalography study. *PLoS One* 7: e50095, 2012. doi:10.1371/journal.pone.0050095.
240. **Liu H**, **Ge H**, **Xiang J**, **Miao A**, **Tang L**, **Wu T**, **Chen Q**, **Yang L**, **Wang X.** Resting state brain activity in patients with migraine: a magnetoencephalography study. *J Headache Pain* 16: 42, 2015. doi:10.1186/s10194-015-0525-5.
241. **Xiang J**, **deGrauw X**, **Korostenskaja M**, **Korman AM**, **O'Brien HL**, **Kabbouche MA**, **Powers SW**, **Hershey AD.** Altered cortical activation in adolescents with acute migraine: a magnetoencephalography study. *J Pain* 14: 1553–1563, 2013. doi:10.1016/j.jpain.2013.04.009.
242. **Kim JA**, **Bosma RL**, **Hemington KS**, **Rogachov A**, **Osborne NR**, **Cheng JC**, **Oh J**, **Crawley AP**, **Dunkley BT**, **Davis KD.** Neuropathic pain and pain interference are linked to alpha-band slowing and reduced beta-band magnetoencephalography activity within the dynamic pain connectome in patients with multiple sclerosis. *Pain* 160: 187–197, 2019. doi:10.1097/j.pain.0000000000001391.
243. **Kisler LB**, **Kim JA**, **Hemington KS**, **Rogachov A**, **Cheng JC**, **Bosma RL**, **Osborne NR**, **Dunkley BT**, **Inman RD**, **Davis , KD.** Abnormal alpha band power in the dynamic pain connectome is a marker of chronic pain with a neuropathic component. *NeuroImage Clin* 26: 102241, 2020. doi:10.1016/j.nicl.2020.102241.
244. **Kuo P-C**, **Chen Y-T**, **Chen Y-S**, **Chen L-F.** Decoding the perception of endogenous pain from resting-state MEG. *NeuroImage* 144: 1–11, 2017. doi:10.1016/j.neuroimage.2016.09.040.
245. **Low I**, **Kuo P-C**, **Liu Y-H**, **Tsai C-L**, **Chao H-T**, **Hsieh J-C**, **Chen L-F**, **Chen Y-S.** Altered brain complexity in women with primary dysmenorrhea: a resting-state magneto-encephalography study using multiscale entropy analysis. *Entropy* 19: 680, 2017. doi:10.3390/e19120680.
246. **Furman AJ**, **Meeker TJ**, **Rietschel JC**, **Yoo S**, **Muthulingam J**, **Prokhorenko M**, **Keaser ML**, **Goodman RN**, **Mazaheri A**, **Seminowicz DA.** Cerebral peak alpha frequency predicts individual differences in pain sensitivity. *NeuroImage* 167: 203–210, 2018. doi:10.1016/j.neuroimage.2017.11.042.
247. **Furman AJ**, **Prokhorenko M**, **Keaser ML**, **Zhang J**, **Chen S**, **Mazaheri A**, **Seminowicz DA.** Sensorimotor peak alpha frequency is a reliable biomarker of prolonged pain sensitivity. *Cereb Cortex* 30: 6069–6082, 2020. doi:10.1093/cercor/bhaa124.
248. **Furman AJ**, **Thapa T**, **Summers SJ**, **Cavaleri R**, **Fogarty JS**, **Steiner GZ**, **Schabrun SM**, **Seminowicz DA.** Cerebral peak alpha frequency reflects average pain severity in a human model of sustained, musculoskeletal pain. *J Neurophysiol* 122: 1784–1793, 2019. doi:10.1152/jn.00279.2019.
249. **Davis KD**, **Aghaeepour N**, **Ahn AH**, **Angst MS**, **Borsook D**, **Brenton A**, **Burczynski ME**, **Crean C**, **Edwards R**, **Gaudilliere B**, **Hergenroeder GW**, **Iadarola MJ**, **Iyengar S**, **Jiang Y**, **Kong J-T**, **Mackey S**, **Saab CY**, **Sang CN**, **Scholz J**, **Segerdahl M**, **Tracey I**, **Veasley C**, **Wang J**, **Wager TD**, **Wasan AD**, **Pelleymounter MA.** Discovery and validation of biomarkers to aid the development of safe and effective pain therapeutics: challenges and opportunities. *Nat Rev Neurol* 16: 381–400, 2020. doi:10.1038/s41582-020-0362-2.
250. **Davis KD**, **Flor H**, **Greely HT**, **Iannetti GD**, **Mackey S**, **Ploner M**, **Pustilnik A**, **Tracey I**, **Treede RD**, **Wager TD.** Brain imaging tests for chronic pain: medical, legal and ethical issues and recommendations. *Nat Rev Neurol* 13: 624–638, 2017. doi:10.1038/nrneurol.2017.122.
251. **Boto E**, **Holmes N**, **Leggett J**, **Roberts G**, **Shah V**, **Meyer SS**, **Muñoz LD**, **Mullinger KJ**, **Tierney TM**, **Bestmann S**, **Barnes GR**, **Bowtell R**, **Brookes MJ.** Moving magnetoencephalography towards real-world applications with a wearable system. *Nature* 555: 657–661, 2018. doi:10.1038/nature26147.
252. **Knappe S**, **Sander T**, **Trahms L.** Optically-pumped magnetometers for MEG. In: *Magnetoencephalography: From Signals to Dynamic Cortical Networks*, edited by Supek S, Aine CJ. Berlin: Springer, 2014, p. 993–999.
253. **Iivanainen J**, **Zetter R**, **Grön M**, **Hakkarainen K**, **Parkkonen L.** On-scalp MEG system utilizing an actively shielded array of optically-pumped magnetometers. *NeuroImage* 194: 244–258, 2019. doi:10.1016/j.neuroimage.2019.03.022.
254. **Mosher JC**, **Baillet S**, **Leahy RM.** Equivalence of linear approaches in bioelectromagnetic inverse solutions. In: *IEEE Workshop on Statistical Signal Processing, 2003*. IEEE, 2003, p. 294–297. doi:10.1109/SSP.2003.1289402.